Journal of Iberian Geology (2024) 50:227–248
https://doi.org/10.1007/s41513-024-00237-x

REVIEW ARTICLE

Saucer blowouts in the coast dune fields of NW Spain

G. Flor[1] · P. Martínez Cedrún[2]

Received: 9 October 2023 / Accepted: 7 April 2024 / Published online: 1 June 2024

Abstract

Three selected stabilized saucer blowouts in the coast of NW Spain (Iberian Peninsula) are studied under the morphological and sedimentological points of view. The morphologies of these blowouts are characterized: rim, crest, deflation bottom, right (inner and outer) and left (outer and inner) flanks, outer windward and inner lee ward flanks, inner windward and outer lee ward flanks. They are slightly elongated according to the main direction of the prevailing wind. From surficial sand samples, isolines of grain-size parameters such as centile, mean, sorting, skewness, and kurtosis, as well as the mineralogical composition (bioclastic carbonate versus siliciclastic percents) have been considered to establish specific trends. In many cases, isoline contours are adapted to the floor and the sedimentary rim, allowing to deduce the main flow of the wind that contributes to their formation and development of the complex geometry including their granulometry and composition. The average size is coarser in the outer windward and deflation bottom, and minimum in the crest; the sorting is better in the outer lee side and moderate on the bottom; the skewness shows no contrast being only extreme in the inner lee side; less sharp curves are represented on the windward and leeward flanks and crest, and are leptokurtic on the leeward side; carbonate percents are maximum on the outer lee ward side, followed by the bottom, being minimum on the inner windward side. The flank slopes are very high in the outer leeward and internal windward, and moderate in the outer windward and flat in the crest and deflation bottom. A simple model of morphodynamic and sedimentary characterization is proposed, under unidirectional winds.

Keywords Saucer blowouts · Morphologies · Grain-size parameters · Trends · Morphosedimentary model · NW Spain

Resumen

Se han seleccionado tres casquetes dunares estabilizados del tipo “saucer blowout” en la costa del NO de España (Península Ibérica) para su estudio bajo las perspectivas morfológica y sedimentaria. Se han caracterizado las morfologías que constituyen estos casquetes: ribete sedimentario, cresta, fondo de deflación, flancos derecho (interior y exterior) e izquierdo (exterio e interior), flancos externo de barlovento e interno de sotavento y flancos interno de barlovento y externo de sotavento. Están ligeramente alargados en la dirección del viento dominante. A partir de muestras arenosas superficiales, se han elaborado mapas de isolíneas de los parámetros granuloméricos: centil, media, calibrado, asimetría y angulosidad, así como de la composición mineralógicala (porcentajes carbonatados bioclásticos vs siliciclásticos) con el objeto de establecer las tendencias específicas. En muchos casos, los contornos de las isolíneas se adaptan al fondo y al ribete sedimentario. El tamaño es más grueso en el costado externo de barlovento y en el fondo de deflación, y mínimo en la cresta; el calibrado es mejor en el costado exterior de sotavento y moderado en el fondo; la asimetría no muestra contrastes, siendo solo extrema en el costado interno de sotavento; curvas menos agudas están representadas en los flancos de barlovento y sotavento y en

✉ G. Flor
gflor@uniovi.es

P. Martínez Cedrún
patricio.martinez@unican.es

[1] Department of Geology, University of Oviedo, C/ Jesús Arias de Velasco, s/n, 33005 Oviedo, Spain

[2] Department of Earth Science and Condensed Matter Physics, University of Cantabria, Avda. de los Castros, s/n, 39005 Santander, Spain

la cresta, y son leptokúrticas en el costado de sotavento; los porcentajes carbonatados son máximos en el costado externo de sotavento, seguidos del fondo, y mínimos en el costado interno de barlovento. Las pendientes de los flancos son muy altas en el costado externo de sotavento e interno de barlovento, moderadas en el exterior de barlovento y planas en la cresta y fondo de deflación. Se propone un modelo simplificado para su caracterización morfodinámica y sedimentaria, bajo vientos unidireccionales.

Palabras clave Casquetes "saucer blowout" · Morfologías · Parámetros granulométricos · Tendencias · Modelo morfosedimentario · NO España

1 Introduction

Aeolian dunes and dune fields owe their formation, fundamentally, to the accumulation of sand, but erosive typologies can be found as the result of intense winds (Hesp, 1999). Erosion processes can be manifested in the formation of basic dunes whose geometries are presided over by depressions of variable contours (Cooper, 1958; Hesp, 2002), erosional scarps (Gares & Nordstrom, 1995) and a deeper deflation basin or depression, as inland transport corridors. They can be accompanied simultaneously by a sedimentation with a positive topography (Abhar et al., 2015) as a downwind depositional lobe and/or a border rim rounding the hollow. The combination of factors such as the previous topography, erosion of the foredune by winds and waves and changes in the vegetation cover could be the triggering factors in the formation of a wind-excavated gap (González-Villanueva et al., 2011).

Blowouts are known since 1898 by Cowles (Hesp, 2002). Basically, two primary typologies are recognized (Cooper, 1958, 1967): saucer blowouts (shallow, short-lived blowouts) and trough ones (much longer-lived and deeper). Also, González-Villanueva et al. (2011) refer to this particularity. Ritchie (1972) defined four types of blowouts including cigar-shaped, v-shaped, scooped hollow, and cauldron and corridor. Hesp (2002, 2011) incorporates another type, named bowl, that acquires a deeper sub-elliptical or semicircular form (Hesp & Walker, 2012; Smyth et al., 2012). Complex blowouts are identified (Carter et al., 1990), and mixed shape and bitten blowouts are developed in the Menorca coast in Balearic Islands of Spain (Mir-Gual et al., 2017). These and other varied blowout morphologies are distinguished by Abhar et al. (2015) and Hesp et al. (2017).

Blows have been considered as former depressions that evolved to parabolic dunes in a vegetated dune surface (McKenna, 2007; Pye & Tsoar, 2009; Sloss et al., 2012). In all cases, they are excavated on sandy deposits sedimented previously in irregular sets with hummocky geometries, with different meaning from those similarly named by Hesp and Thom (1990) as coppice dunes. However, they are usually associated with the crests of active foredunes or on the windward side (Smith, 1960) if they are elongated. These hummocky fields have been categorized as collision dunes, which were stabilized to become a topography of residual type, according to a vegetation-dune interaction model (Barchyn & Hugenholtz, 2012), without involving other defined typologies. Foredune blowouts are erosional features that allow aeolian flow-through of sand from the beach into the back dunes; their evolution reflects the aggregation of both environmental (abiotic) and ecological (biotic) (Schwarz et al., 2019).

In simple terms, hollows have the shape of a flat dish (saucer) and grow according to the wind flow (Thomas, 2004), and can be exclusively erosive or construct a sedimentary rim, bordering the perimeter of the depression. Even a depositional lobe or fan (fan-like blowover "delta") (Carter et al., 1990) can be formed, that is constructed to leeward in external position (Glenn, 1979; Hesp, 2002). Their plant is more usually sub-elliptical, but also semicircular, which is completed by a sub-plane or hemisphere bottom that represents a space of deflation (deflation basin by Hesp, 2002). The crest of the border serves as a dividing line between the outer and inner slopes, of erosive character (erosional walls by Hesp, 2002), which acquire greater angles of inclination. In some cases, the slopes of internal flanks, mainly in the larger blows, are so steep that they favor the formation of irregular avalanches, along which granular flows occur (Tripaldi, 2001).

The sub-elliptical ones are numerous in Spanish NW coasts and even more in the Galicia cases of Frouxeira, San Jorge, Barra do Medio and Traba (Fig. 1). Pérez Alberti and Vázquez Paz (2011) highlight the existence of active elongated depressions on the windward side of the great dune of Corrubedo in different records of its evolution, controlled from 1998 to 2008. They are relatively scarce in Cantabria, and they can be identified in the climbing dune field of Liencres (Martínez Cedrún & Flor, 2008), where they acquired very clear geometries, and in the Puntal of Somo and Laredo, Noja and Sonabia (Fig. 1). In Asturias, some blows were formed on the windward side of the Salinas-El Espartal foredune. They were eroded and disappeared towards the 80s (Flor, 2004; Flor et al., 2019).

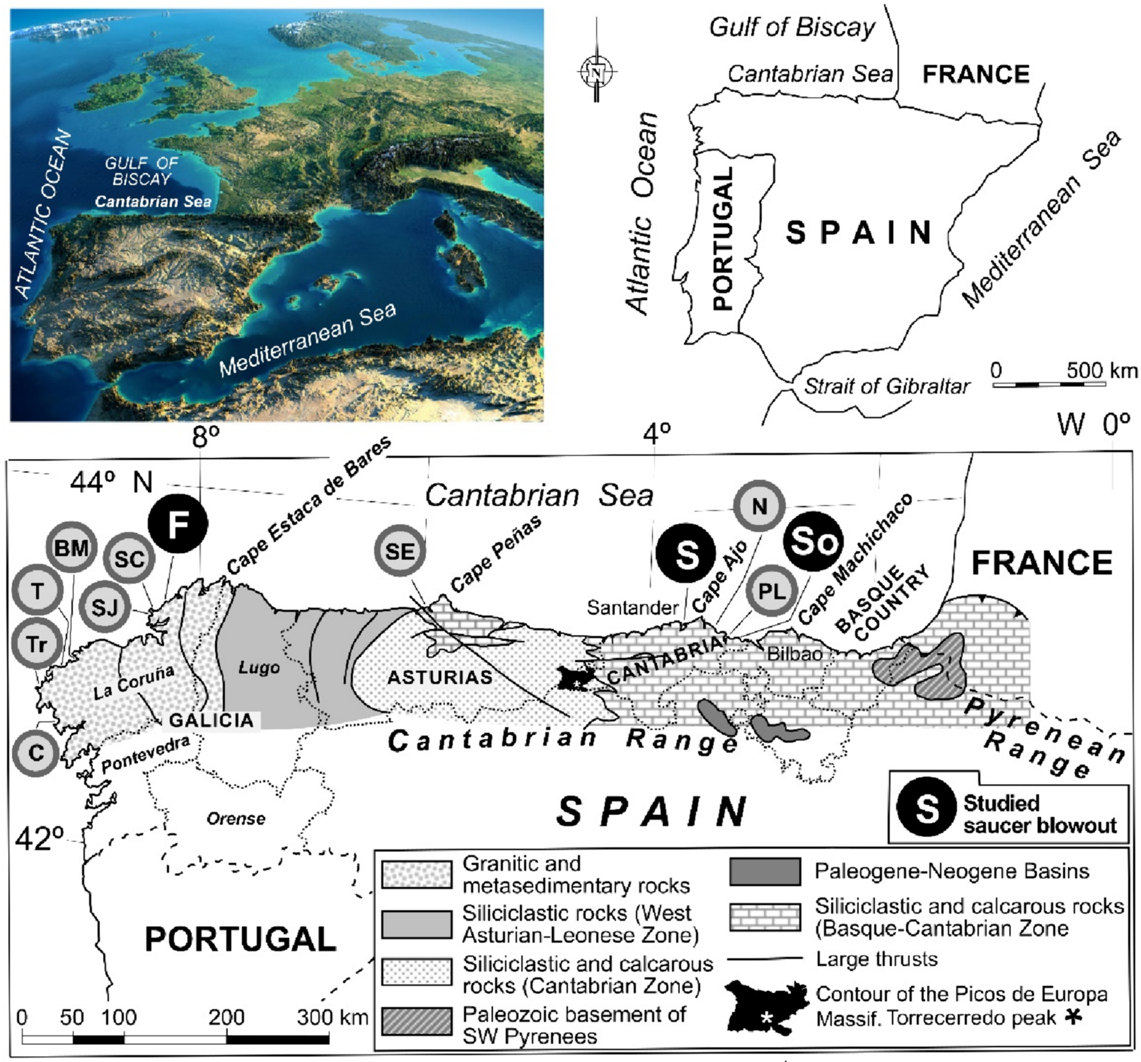

Fig. 1 Situation of the studied blowouts (black circular background) along the NW coasts of Galicia (Frouxeira-F) and central (Somo-S) and east (Sonabia-So) of Cantabria, and other aeolian dune fields mentioned in the memory. On gray circular background: Corrubedo-C, Traba-Tr, Trece-T, Barra do Medio-BM, San Jorge-SJ, Santa Comba-SC, Salinas/El Espartal-SE, Noja-N and Puntal de Laredo-PL. Simplified tecto-stratigraphic regions of the Pyrenean-Cantabrian system and Galician igneous rocks, mostly granitoids (modified from Fillon et al., 2016). (*) Maximum height of the Picos de Europa Massif

The subspherical blowouts have been studied from the perspective of their morphology (Jungerius & van der Meulen, 1989; Thomas, 2004), morphological evolution over time (Hugenholtz & Wolfe, 2009; Jungerius et al., 1981; Smith et al., 2017) in what would represent a continuous sequence from subspherical to elongated blows (Davidson-Arnott et al., 2019; Hansen et al., 2009; Hesp & Pringle, 2001). In this case, they construct a lobe or prograding prism downwind, and the dynamics of wind flows (Hesp & Hyde, 1996; Jungerius & van der Meulen, 1989; Hugenholtz & Wolfe, 2006, 2009; Hesp & Walker, 2012; Smith et al., 2017; Hesp et al., 2017).

Blowouts commonly grow in length upwind against the prevailing wind (Abhar et al., 2015). Intense winds contribute to the formation of elongated blows, where the most energetic turbulence characterizes these excavated areas on the windward sides (Kolm, 1982). Trough blowouts are opened perpendicular to the water line obliquely, well represented in the beaches of Traba, O Trece and, also, in Frouxeira and Santa Comba, in this case coexisting with parabolic ones (Flor, 1992). They have been much more studied from the aerodynamic perspective (Hesp & Pringle, 2001; Hugenholtz & Wolfe, 2006; Mir-Gual et al., 2013, 2017) than the saucer blows.

In Galicia, the internal structure of the sandy sedimentation in sub-elliptical and elongated blows has been detailed by georadar (González-Villanueva et al., 2011) and the temporal evolution (González-Villanueva et al., 2013) in the beach/dunes of Traba (Fig. 1).

This paper is one of the few detailed studies dedicated to the sedimentologic point of view of three saucer blowouts mainly erosive of the coastal dune fields developed in Galicia and Cantabrian Sea. The selected blows in this research, with very different geographical locations and geological contexts, have provided many data that allow obtaining general and particular behaviors that can be extrapolated to others of similar characteristics. The distribution of granulometric parameters and siliciclastic vs. biogenic carbonate contents (%) has been drawn through trend isoline maps. They provide information on the sedimentation regarding the characterization of the different morphologies, and the possibility to deduce from the prevailing winds, including the morphological content, the dynamic patterns. This study fundamentally focused on granulometric variables are essential to complete the knowledge about the dune morphology, sedimentary transport and the dynamic model in these blow typologies.

2 Study site

The steep coasts of the northwestern Spain (Iberian Peninsula) are developed in a mountain relief that, from Asturias to Basque Country, is represented by the Cantabrian Range, wich is approximately 350 km long, with highest peak of 2649 m (*) in the Picos de Europa Massif (Fig. 1). It is parallel to the Cantabrian coastline in an east-west direction and descending northward to the coast with a width of over 30–50 km. Thus, the fluvial network is short and steeply sloped, but with a great erosive power; fast-owing run essentially perpendicular to the coast, carving a series of steep valleys. It was uplifted during the orogenic phases of the Alpine Cycle, triggering the formation of continental erosion surfaces and up to 12 levels of stepped coastal ones (Flor & Flor-Blanco, 2014a). The cliffed coast of Galicia is the most indented stretch of Spain with a succession of flooded valleys, the rias, drowned from the Holocene. This is an ancient bedrock of granitic and metasedimentary rocks in the Atlantic margin of the Iberian Peninsula and has a strong geostructural control (Pérez-Alberti et al., 2013). The littoral of Cantabria is developed in the Cretaceous Basque-Cantabrian basin (Feuillée & Rat, 1971), containing rock outcrops of Triassic age, highlighting evaporites and episodic volcanic rocks, where limestones have a greater representation.

The climate is temperate-humid, represented by the *Cfa* and *Cfb* climatic types of Köppen-Geiger in the Galician and Cantabrian coasts, respectively (García Couto, 2011). The river basins are net suppliers of siliciclastic sandy fractions to the coast, via estuaries in the Cantabrian coast, and rias in Galicia (Flor et al., 2022; Flor-Blanco & Flor, 2019). Carbonate bioclastic sands derive from processes of coastal upwellings, and the output of nutrient supplies from estuaries and rias with extensive muddy plains and marshes to the peritidal rocks (Flor et al., 1982). In the Galician coasts, the cliffs contribute with the erosion and emptying of layers of alteration, mainly in granites (Pérez Alberti & Vázquez Paz, 2011). The mineralogical components can be inherited from previous eustatic stages (Roy & Thom, 1981), particularly in the case of carbonate bioclasts on the coasts of the Cantabrian Sea (Fernández-Valdés et al., 1994; Flor-Blanco & Flor, 2019).

Regarding the aeolian regime, wind is the exclusive dynamic agent to deflate the beaches, transport and store the sandy fractions, constituting the dune fields. It is well documented that wind is the major driving force behind blowout development (Bolles, 2012).

There is a strong spatial variability, with Galicia being the windiest. Seasonal directional changes are noticeable and large dispersion are subject to high seasonality (Lorente-Plazas et al., 2015). In these northwestern coasts of Spain, the winds come predominantly from the S and SW in winter (Fig. 2B, C), acting previously to the passage of Atlantic rainy fronts, and are characterized by being dry and intense. They are followed by the NE winds (Fig. 2B, C), also dry and intense, typical of anticyclonic conditions (summer), contributing to the formation of coastal upwellings (Lavín et al., 2004). Those of the W, best formed in eastern Cantabrian coast (Fig. 2D), are humid and of certain intensity (winter); the frequencies of the winds of the W and NW are maintained in intermediate values throughout the year that coincide with the precipitations in the Bay of Biscay (Felicísimo Pérez, 1992).

These wind components (Fig. 2), together with the orientation and orography of the coastal segment in each case, more sharply in Sonabia (Fig. 2D) than in Frouxeira (Fig. 2B), are isolated or combined inducers of the opening and development of these erosive and sedimentary forms of wind character. The blowouts of Frouxeira and El Puntal are opened by NE winds, and the blow of Sonabia by NW components, probably with the dependence of the surrounding relief, located in the western side where the calcareous Candina massif emerges NW–SE with heights of 486 m.

This wide dissipative beach of Frouxeira (Figs. 1, 3A, B) is located in the NE of Ferrol, province of La Coruña (Galicia). It draws an arched plan at NNE with a length of 2.58 km and 275 m wide. It hosts a relatively broad dune field of 198 ha, which is extended further towards the S on the areas dedicated to pastures, crops and eucalyptus, and to the W and NW. Backbeach dunes are constituted by an active field (a maximum width of 170 m) that is migrating landward and are represented by irregular vegetated dunes, tongue-like dunes, sand shadows and wrap-around dunes,

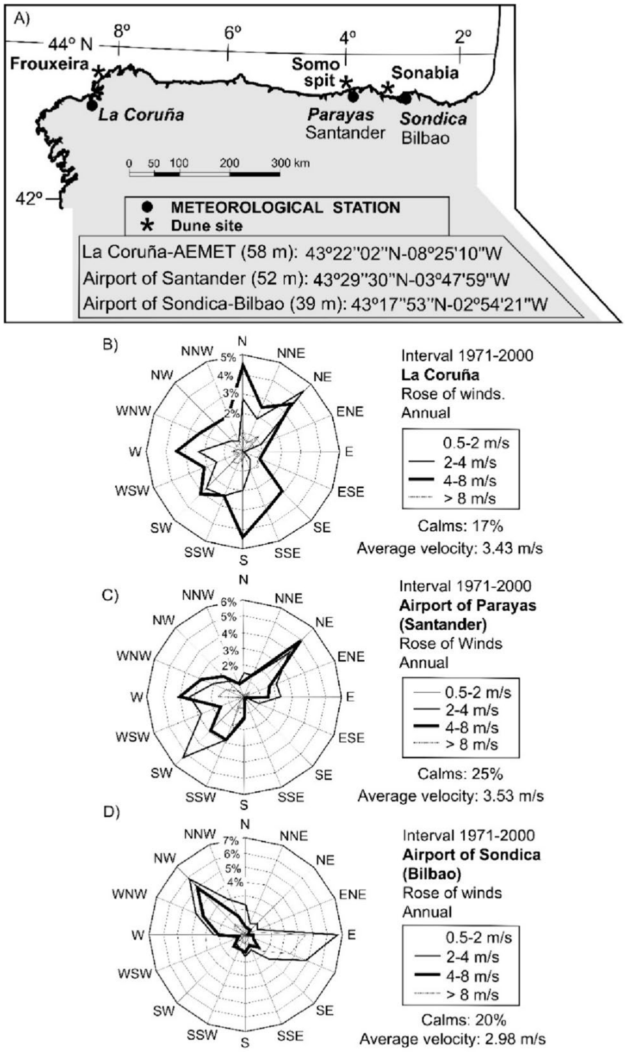

Fig. 2 **A** Situation of the meteorological stations, including the elevation (m) and geographic coordinates, from which the annual wind data has been obtained: wind roses (frequency in % and average velocities in m/s). They are applied to each of the nearest dune fields: La Coruña (**B**), center Cantabrian coast in the airport of Parayas-Santander (**C**), and airport of Sondica-Bilbao in the eastern coast of Biscay (**D**) from Pinazo Ojer (2010)

tabular sheets, residual knobs, and sub-elliptical and elongated blowouts (Fig. 3A, B), both with and without sedimentary lobes. Broad and irregular deflation surfaces are developed somewhere in the field and narrow corridors from the upper beach. Eroding remnant knobs, nebkhas, climbing and cliff-top dunes formed towards the sides W and NW, where numerous deflation basins have been opened and blowouts. Beach and foredune sands (29.34 and 18.75 bioclastic carbonate percent, respectively) are medium grain-sized and climbing dunes (2.90 carbonate percent) are fine sands (Flor, 1984, 1992; Flor et al., 1983).

Foredunes are preserved at the NW end of the beach, with vegetation of European marram grass (*Ammophila arenaria*) being replaced towards the center and east areas by embryonic sheets of sand couch grass (*Elymus farctus*).

The sandy spit of Somo constitutes the confining barrier of the Santander Bay (Figs. 1, 3C), within which two estuarine subsystems are identified (Flor & Flor-Blanco, 2014b). It has a length of 2.55 km on top of which vegetated dunes culminate (Martínez Cedrún, 2009). These occupy a belt of about 28.85 ha with varying widths, larger on the eastern side (320 m) to decrease irregularly with an average of 75 m. The grain sizes of beach sands are medium decreasing slightly in the dunes and biogenic carbonates are 27.5% and 25.69%, respectively (Martínez Cedrún, 2009).

It is crossed by many corridors of wave erosion, most of them artificially filled and revegeted with marram grass (*Ammophila arenaria*), but some of them are functional, such as the edge near the town of Somo, which has built a double sedimentary lobe (washover fan) on the estuarine environment during the 2014 storms (Flor & Flor-Blanco, 2016); other active corridors are open in the westernmost segment of the barrier, highlighting, in addition, the wide area of deflation in the vicinity of the Rabiosa Point as a result of the ongoing construction of the spit migrating westwards, still unvegetated (Fig. 3C).

The dune field is represented by foredunes in the exposed (N) and estuarine (S) sides, as well as saucer blowouts and tongue-like dunes inside of the spit. During the last decades, the reduction of the dune width and the migration of the spit towards the W (inside the subsystem of Santander), studied by some authors (de Sanjosé et al., 2017, 2018, 2021; Flor & Flor-Blanco, 2016; Losada et al., 1991), has promoted the disappearance of the main body of original foredunes and the opening of new corridors, transversely to the spit.

This narrow embayed beach of Sonabia and its wide aeolian dune field, that occupies 11 ha, are located in a bay of an elongated triangular plant, whose axis is oriented NW–SE in a length of about 650 m and widths of 120–150 m respect the spring low-water tide (Fig. 3E). Most of the dune field is represented by a complex of barchans and longitudinal dunes (Flor & Martínez Cedrún, 1991), drawing an orthogonal hatch in plan that was formed in past times and totally inactive due to the fixation by vegetation (Fig. 3F).

Backside the beach, an active foredune and two saucer blowouts (Fig. 3E), both fully vegetated (Fig. 3G), just landward are developed. Beach and dunes sands are fine-grained: 2.25φ (0.21 mm) and 2.32φ (0.20 mm) and biogenic carbonates are 73.5% and 73.22%, respectively (Martínez Cedrún, 2009). Elorza and Higuera-Ruiz (2015) carried out a calcimetric analysis of the Sonabia sands in the beach and climbing dunes in which they obtained slightly lower average values.

Three blowouts that are not affected by wave storms were selected (Fig. 1) without any sedimentary lobe: Frouxeira (F) in northeastern Galicia (Fig. 3A, B), Somo (S) and Sonabia

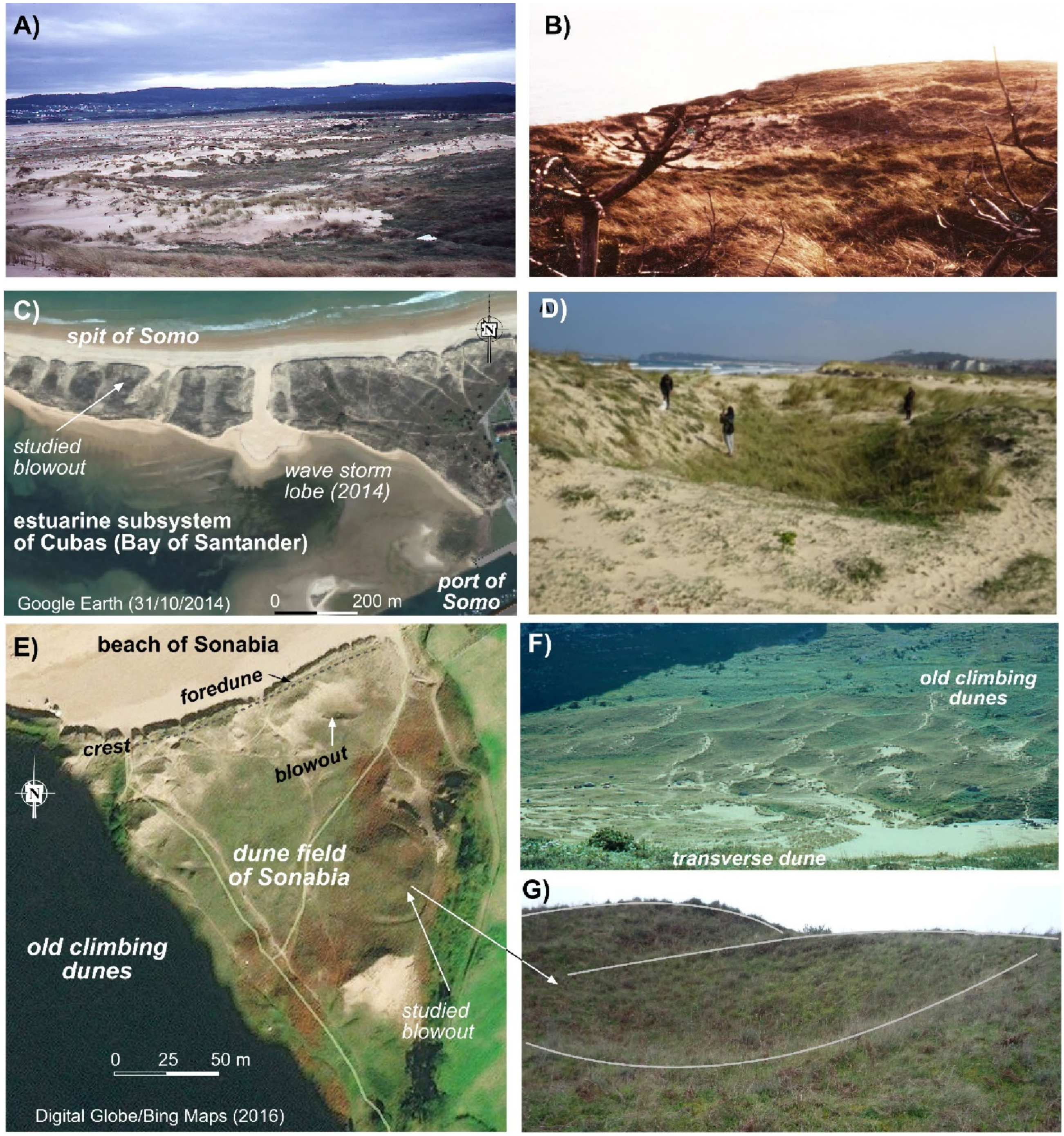

Fig. 3 **A** Active dune field of Frouxeira, constituted by trough blowouts and downwind elongated lobes migrating landward. **B** A saucer subeliptic blowout that was opened in the climbing dune sheet of Frouxeira, partially stabilized by vegetation of *Ammophila arenaria*; the mainwind (NE) comes from the left side. **C** Sand spit of Somo viewed from the SW side where the studied blowout is developed. **D** View of the blowout of Somo from the western to eastern side, highly colonized with *Ammophila arenaria*. **E** Aeolian dune field of Sonabia where the foredune is retraiting, and location of the sudied blowout; the old climbing dune field is in shadow slope. **F** View from the eastern side of the calcareous massif of Candina that is elongated NW–SE and, in the foreground, the inactive field of climbing dunes: barchan and transverse dunes; Sonabia beach is in the lower right corner. **G** A view from the innermost transverse dune towards the beach, in whose foreground the studied saucer blowout is distinguished, which is fixed by a dense vegetation cover; the contours have been highlighted with light gray lines

Table 1 The class intervals of the granulometric parameters applied to draw the contour diagrams (F&W = Folk & Ward, 1957)

Mean sizes	0.00–1.00 ϕ (1.00–0.50 mm): *coarse sand*	Sorting or standard deviation (F&W)	< 0.35 ϕ: *very well sorted*
	1.00–2.00 ϕ (0.50–0.25 mm): *medium sand*		0.35–0.50 ϕ: *well sorted*
	2.00–3.00 ϕ (0.25–0.125 mm): *fine sand*		0.50–1.00 ϕ: *moderately sorted*
	3.00–4.00 ϕ (0.125–0.0625 mm): *very fine sand*		1.00–2.00 ϕ: *poorly sorted*
Skewness (F&W)	− 1.00 to (− 0.30): *very negative*	Kurtosis (F&W)	0.67–0.90: *platykurtic*
	− 0.30 to (− 0.10): *negative*		0.90–1.11: *mesokurtic*
	− 0.10 to (+ 0.10): *almost symmetrical*		1.11–1.50: *leptokurtic*
	+ 0.10 to (+ 0.30): *positive*		1.50–3.00: *very leptokurtic*
	+ 0.30 to (+ 1.00): *very positive*		> 3.00: *extremely leptokurtic*

(So) in central (Fig. 3C, D) and eastern coast (Fig. 3E, F) of Cantabria, respectively; the blowout of Somo (Fig. 3D) and the entire one of Sonabia are completely vegetated (Fig. 3F). Although blowouts are considered as erosional features in costal aeolian landscapes, these are representative of mixed erosive and with simple sedimentary rims, partially or totally, with single (Frouxeira) or complex bottoms (Somo and Sonabia). In addition, the Somo blowout can be considered as a bowl, being the evolutionary result a sub-elliptic saucer one.

3 Methodology

The applied methodology, simplified from Hesp et al. (2016), consisted in a topographic survey of each saucer blowout using a digital clinometer (accuracy of 1/10 degree), recording the angles of inclination, and tape measure with the help of a laser distance meter. In addition, new measurements were made applying the Emery method of beach profiling, using stakes, each one has a measurement scale graduated every 10 cm and using the Compass of Meridian attached on a tripod. Several transect lines along and across each blowout were established and surveyed, supplemented with short profiles and additional sampling of surficial sands. To characterize them morphologically, the significant geometries are detailed: rim, crest, deflation bottom, right (inner and outer) and left (outer and inner) flanks, elongated according to the direction of the wind, downwind, outer windward and inner lee ward flanks, and inner windward and outer lee ward flanks.

The historical ortophotos of coasts of Galicia and Cantabria has been consulted selecting those of the highest quality within the second decade of the twenty-first century. That one of Frouxeira in 2017 (IGN) allowed the transgressive dune field to be mapped. Sonabia was recorded in 2016 (Digital Globe Bing Maps) and the dune field of El Puntal of Somo is dated in 31 of November of 2014 (Google Earth).

Representative sandy surface samples were taken for sedimentological characterization; sand fractions were mechanically sieved at intervals of 0.50φ, determining by means of the program Gradistat (Blott & Pye, 2001) the graphic statistical grain-size parameters of centile-C (coarsest percentile, 1%) and mean-Mz, sorting-σ_I or standar deviation, skewness-Sk_I and kurtosis-KG, according to Folk and Ward (1957).

The class intervals are applied according to the proposal of Wentworth scale for the mean sizes (sand grades) and Folk and Ward (1957) for standard deviation or sorting, skewness and kurtosis (Table 1). The centile can be considered like the mean size and carbonate percent trends must be adapted to the results, either at intervals of 5% or 10% and, in same cases, intermediate.

The dominant mineralogical silica-carbonate (biogenic) relation, simplified to this last component, was determined by the volumetric method (Bernard's calcimeter) on the totality of each sample. The grain size is closely related to the carbonate content, since the larger the grain size, the higher the carbonate percentage in beaches and coastal dunes (Flor et al., 1982, 2022; Flor, 1981a).

The results of each grain-size parameter and the carbonate percentages have been shown through isolines in trend maps (sorting and kurtosis with the class intervals proposed by Folk & Ward, 1957) in order to characterize each environment and establish the subordination of a dominant component of wind.

4 Results

These aeolian blows are currently partially or totally inactive and have preserved their morphology and sand content intact.

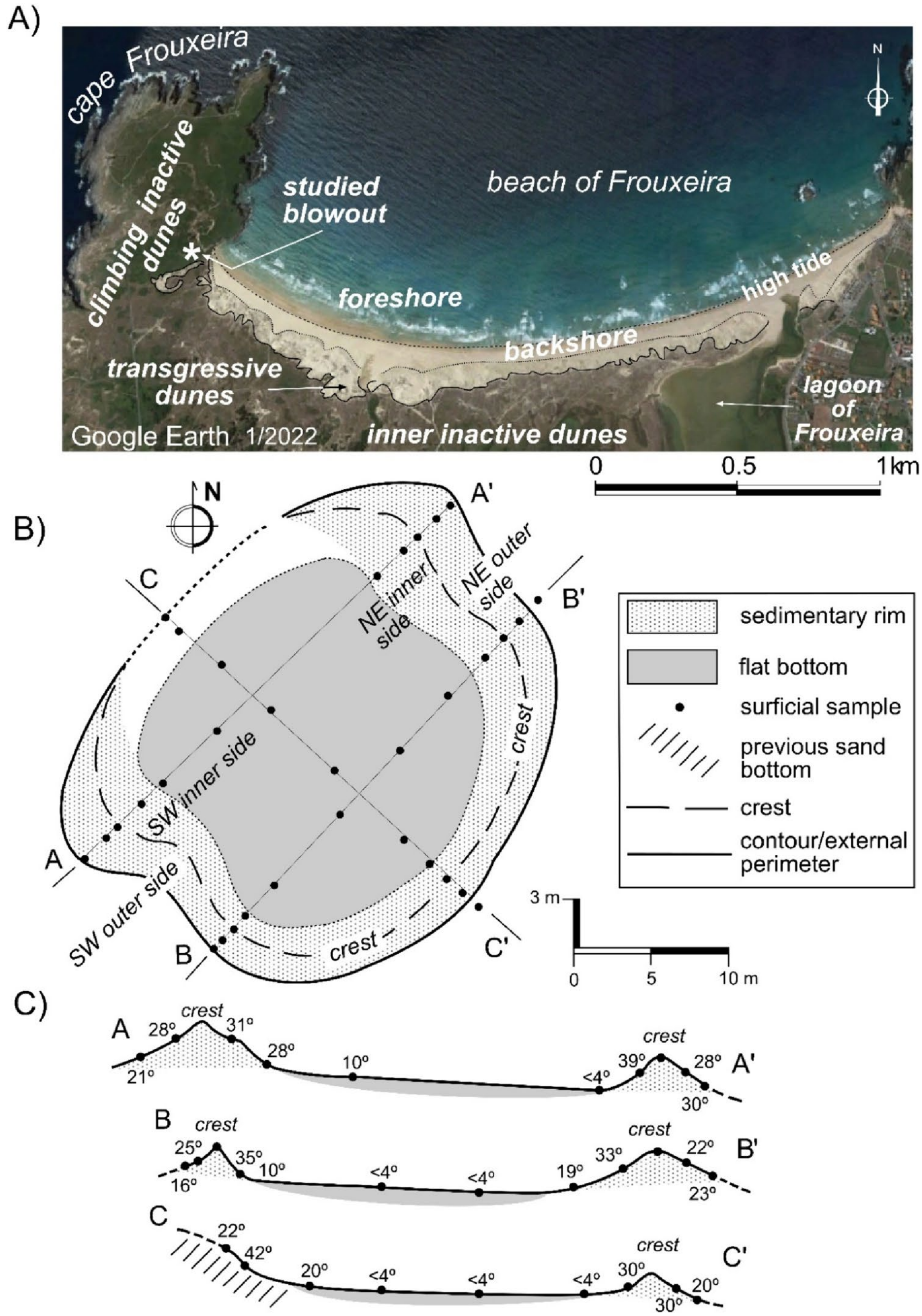

Fig. 4 **A** Mapping of the aeolian dune fields of Frouxeira, highlighting the transgressive dune belt surrounding the upper beach. **B** Morphological reconstruction in plan and transverse profiles where the position of the superficial sandy samples is included. **C** Transverse profiles including detailed slopes, sand sample locations and crests and flat bottoms, obtained from Flor (1984)

4.1 Frouxeira

At the western end of the beach, within a previous sandy deposit that has been emplaced as a climbing and cliff-top dune (Fig. 4A) of tabular character, numerous wind erosion depressions have been formed. At the end of the rocky bar formed by Cape Frouxeira, S and SW winds have activated, developing a series of very complex, with a concentric trend, deflaction basins (some of which are more than 500 m long), and that do not exceed 3 m in height; they are distributed according to an arched plan, convex towards the N and, in its southern edge, a band with moderate deflation is activated (Fig. 4A). It is in this set and in the back strip of the beach, where the aeolian dunes are vegetated and numerous sub-elliptic contours have been developed (Figs. 3B, 4A).

A blowout with an incomplete sedimentary rim was selected for this study; it culminates by a ridge that reaches heights of up to 3 m; the flat bottom has a slope of less than 4° marked by the position of the water table, and it occupies the largest surface; the NW side has been excavated on the

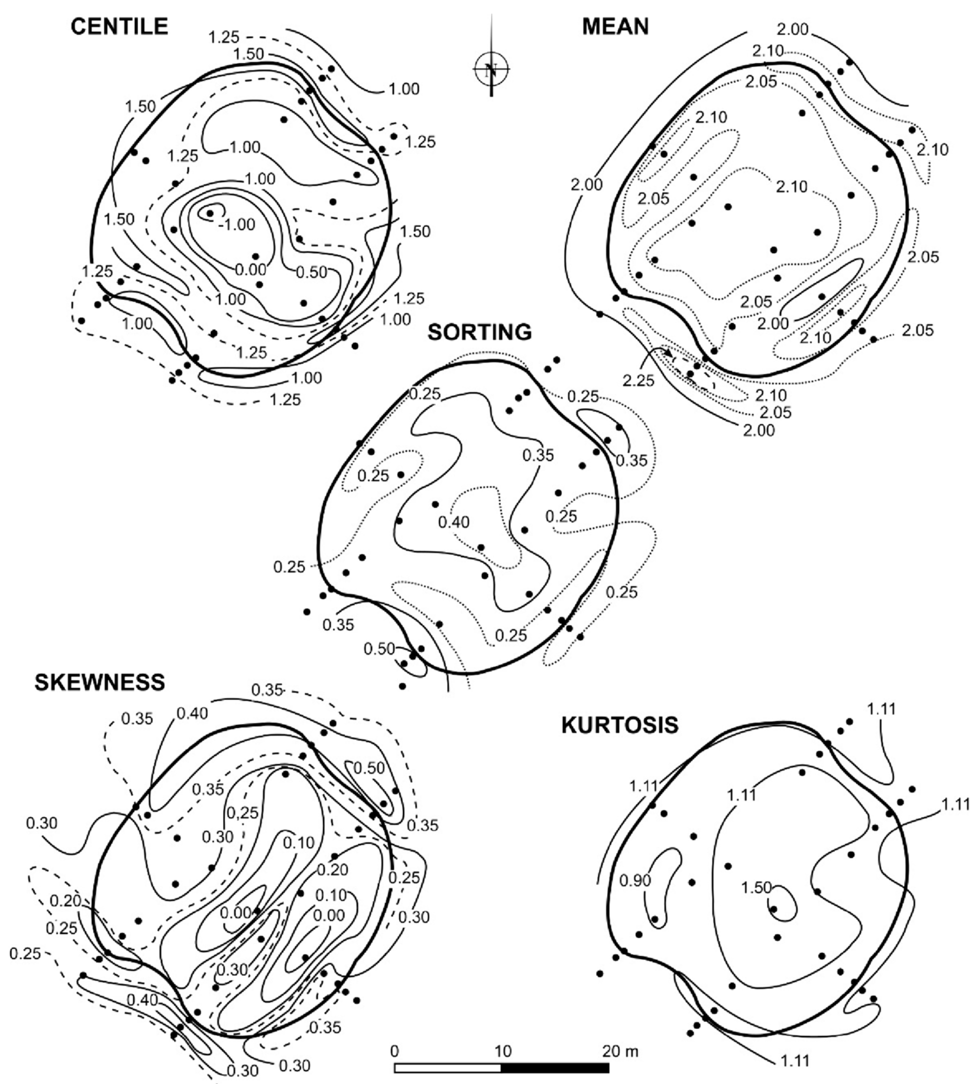

Fig. 5 Trends maps of the grain-size parameters: centile, mean, sorting, skewness and kurtosis in the saucer blowout of Frouxeira

sandy substrate of the tabular climbing dune, which is part of the lower slope (Fig. 4B).

This blowout has a flat bottom with a sedimentary rim of variable widths from 3.40 to 7.35 m; it stretches in the NE-SW direction with 34.5 m, the width (minor axis) is 27 m, and altimetric differences are higher than 3.5 m. The rim develops relatively high slopes, either with similar inclinations (30°) on both sides of the crest, but smaller on the outer and maximum flanks (less than 39°) on the entire inner belt. NE outer side is windward, and SW outer side is lee-side; and southeast segment is the left flank (Fig. 4C).

The grain size ranges from medium to fine sand and are very well sorted. The centile, which is representative of the maximum grain size (maximum kinetic energy of the wind), shows coarser sizes in the SW half of the bottom of the blowout, while they are minimal (1.50φ) in the segment of the NE and SE ridge, followed by the SW (Fig. 5).

These same tendencies are reproduced in the case of the main size (medium kinetic energy), but with more smoothed distributions (Fig. 5). The sorting is worse in the bottom (higher wind intensity with very contrasted energies) and the best (0.25φ) are concentrated in the upper part of the sedimentary rim, which occupy a greater belt in the third NW, except in the SSW corner with a value of 0.50φ (Fig. 5).

The asymmetry trends are relatively irregular, although they are more symmetrical in the southern half of the bottom and highly positive along the sedimentary rim in the outer NE and SW flanks (+ 0.40). The peaked curves (1.50) are concentrated almost in the central position of the bottom, although the categories of sharp curves dominate almost the whole structure (1.11) and normal-flat curves (0.90) in the inner corner of the NW flank (Fig. 5).

The characterization of each morphological unit, through the average data (Table 2), shows a greater contrast in the centiles, revealing areas of greater relative sizes, indicative of strong energy, as is the case of the bottom of the blowout (0.67φ); the same distribution happens in the outer NE flank (0.99φ) where the wind component of the NE acts on its first

Table 2 Maximum, minimum and average values of the grain-size parameters and angles of inclination for each particular morphology of the saucer blowout of Frouxeira

	GRAIN-SIZE PARAMETERS										Angle of inclination	
	Centile (ϕ)		Mean (ϕ)		Sorting (ϕ)		Skewness		Kurtosis			
	maximum	minimum	maximum	minimum	maximum	minimum	maximum	minimum	maximum	minimum	maximum	minimum
CREST	1.02	1.53	2.01	2.16	0.24	0.28	0.15	0.39	0.91	1.25	4°	
	1.23		2.07		0.26		0.28		1.09			
FLAT BOTTOM	-1.10	1.37	1.93	2.11	0.23	0.36	-0.09	0.36	0.91	2.04	3°	
	0.67		2.05		0.29		0.23		1.21			
N WINDWARD	1.51	1.43	2.02	2.12	0.25	0.27	0.16	0.39	0.94	1.14	42°	33°
	0.99		2.07		0.27		0.30		1.01		30°	
S WINDWARD	1.00	1.28	2.00	2.37	0.25	0.51	0.25	0.46	0.92	1.20	30°	15°
	1.12		2.09		0.30		0.31		1.04		22°	
N LEEWARD	1.03	1.40	1.99	2.17	0.24	0.34	0.23	0.54	0.95	1,19	30°	22°
	1.25		2.07		0.27		0.42		1.08		26°	
S LEEWARD	1.13	1.52	2.05	2.12	0.26	0.27	0.23	0.28	0.89	1.03	33°	28°
	1.33		2.08		0.27		0.26		0.97		31°	

contact with the blowout; nevertheless, differences in the parameter of the mean size are scarce.

Standar deviations are relatively worse in the first case (0.29φ) and in the inner NE flank (0.30φ), once the crest is exceeded, which shows the best value (0.26φ). The curves are positive, much higher on the inner SW flank (0.42), where the NE wind arrives frontally after crossing the blowout; the flat bottom is represented by the minimum values of the skewness (0.23). The sharpness of the curves is very variable, from tending to flat on the outer SW flank (0.97), but they follow very closely the outer and inner NE flanks (1.01 and 1.04), to very sharp (maximum at the bottom: 1.21).

Flank slopes are variable (Table 2), being the deeper side where the wind blows frontally against the inner surfaces of the blowout (N windward and S leeward sides) due to the strong windflow circulation; so, highly turbulent flow can be developed around the inner walls. In the NE inner side (A-A' tranverse profile in Fig. 4C) near the crest, a superimposed excavation can be deduced probably generated by a removal including the acceleration of the airflow toward the crest (Gares & Pease, 2014). Besides, near the deflation bottom, airflow accelerates up to the rim (Hugenholtz & Wolfe, 2009).

4.2 El Puntal (Somo)

The studied blowout (Fig. 6A) is slightly elongated NE-SW along 26.5 m and it is completely bordered by a sedimentary rim of height not exceeding 3.5 m (Fig. 6B). The width is 21 m and the minimum width of the sedimentary rim on the northern side is 1.45 m, gradually increasing towards the SE (3.63 m), S (3.90 m) and it is maximum on the SW side (6.54 m). The inner enclosure is constituted by a shallow, almost sub-elliptic depression inside which a bowl-shaped morphology of 3.9 m radius has been excavated; slopes are subvertical escarpments on the NW and SE flanks (greater than 60°), reaching a depth of about 3.5 m from the bottom of the previous one. It was clearly overdeepened in the central area of the depression (Figs. 3D, 6B, C).

The average grain sizes are included between medium and fine sands with variable sorting. The distribution of the grain-size parameters on the blowout (Fig. 7) is similar to that of Frouxeira with maximum sizes in the western center (−0.75φ and 0.50φ) and minimum in the rim at N and S (0.75φ and 1.00φ). The tendencies of the mean show differences according to the axes of the ellipse; they are maximum at the bottom of the depression (1.50φ), increasing in the major axis and finer values towards the SW (2.00φ) and staying towards the E (1.50φ); towards the N and S, the medium sands become thinner, much more towards the NW corner (2.25φ).

Sorting values are the worst in a small area of central western of the bottom (0.75φ), improving towards the SW flank (0.35φ) and to the N (0.375φ), roughly radial. The curves are more negative skewed in the bottom of the hollow (minimum of −0.40) in the northern half, decreasing

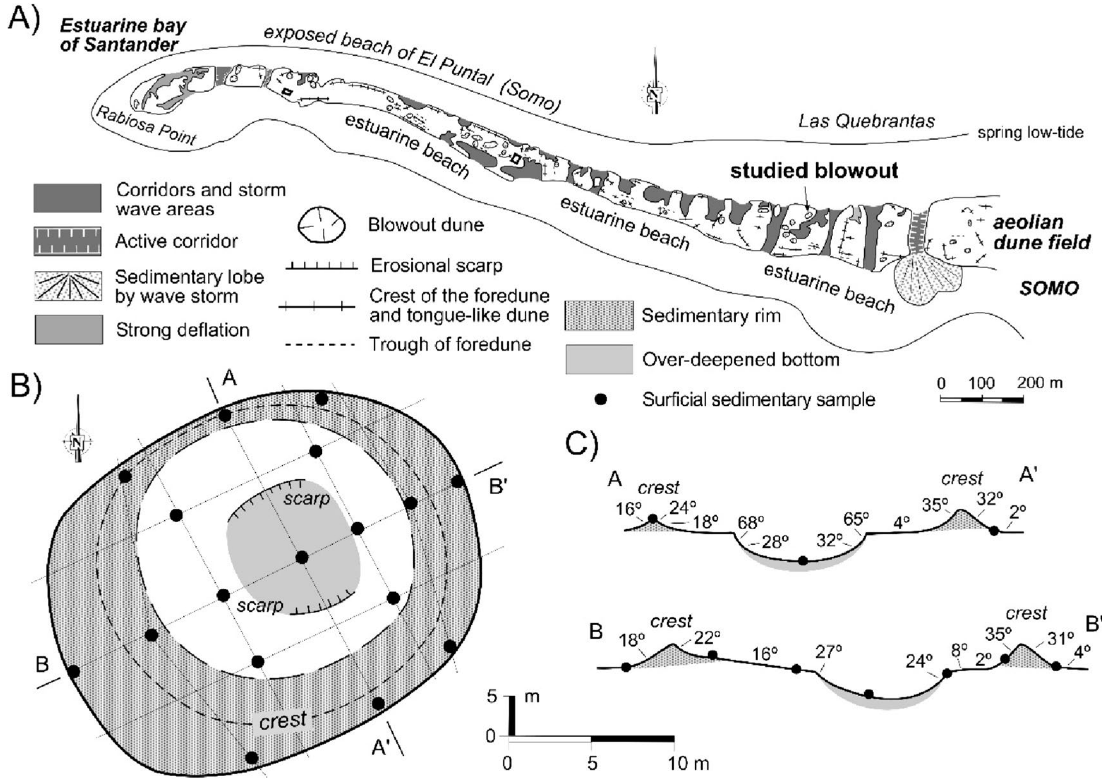

Fig. 6 **A** Situation of the studied blowout in the sandy spit of El Puntal of Somo, including the mapping of the most important morphologic parameters. **B** The slightly elongated blowout has developed a sedimentary rim (gray) and its corresponding crest, inside which the sand substrate was excavated and is characterized by the formation of scarps and the sub-flat bottom. **C** Transverse topographic profiles have been made detailing the position of the surface sandy samples, which have been sedimentologically analyzed. They reveal the geometry of this complex blowout

in the southern half over the sedimentary rim (minimum of -0.20); the curves approach symmetrical in the western third and in the NE and SE corners. The kurtosis reproduces an almost radial distribution from the bottom of the depression with more acute curves (1.75) to medium (1.11) according to an imaginary WNW-ESE axis and flat (0.90) according to another NE–SW axis. The carbonates are maximum at the bottom of the blowout (75%) and at the eastern end (85%), decreasing more or less uniformly at low levels of 10–12.5% towards the NW, and SW, followed by the S (25%).

The averaged grain-size parameters characterize the different morphological and dynamic parts of this subeliptic blowout of the Somo spit well (Table 3). The centile is maximum on the western outer flank (− 0.07φ = 1.95 mm), a residual deposit generated by the SW wind to activate the windward flank of the rim; they are also high on the outer NE flank (0.48φ = 0.72 mm), and inner SW flank (0.52φ = 0.70 mm), as well as on the bottom (0.48φ = 0.72 mm). The crest (1.60φ = 0.33 mm) and the inner NE flank (0.96φ = 0.51 mm) contain the finest sizes. The means offer less contrasted values, but in accordance with those specified for the centile. The sorting, on the other hand, is the best on the outer NE side (0.20φ) where the most selected sedimentary load arrives after having crossed the entire blowout; it tends to be very good on the inner NE flank and the crest (0.39φ). They are relatively worse in the outer SW flank (0.51φ) and in the bottom and inner SW flank (0.46φ), where the agitation is greater.

The skewness is very contrasted, from the exceptional positive value on the crest (0.06), to the most negative (− 0.15), representative of the inner SW flank, followed by the bottom (− 0.11); the rest of the numbers approach the symmetric curve (− 0.01 to − 0.05). The curves range from mesokurtic on the crest (0.94) to acute on the bottom (1.21) and very sharp on the inner SW side (1.94). The percentages of biogenic carbonate are very variable, with a maximum in the outer NE flank (45.77%), probably due to the intervention of NE winds, followed by the bottom (41.42%), both in response to the greater developed energy; it is important, but much smaller on the inner NE flank (25.40%), crest (19.45%) and on the outer and inner SW flanks (14.90% and 12.90%, respectively).

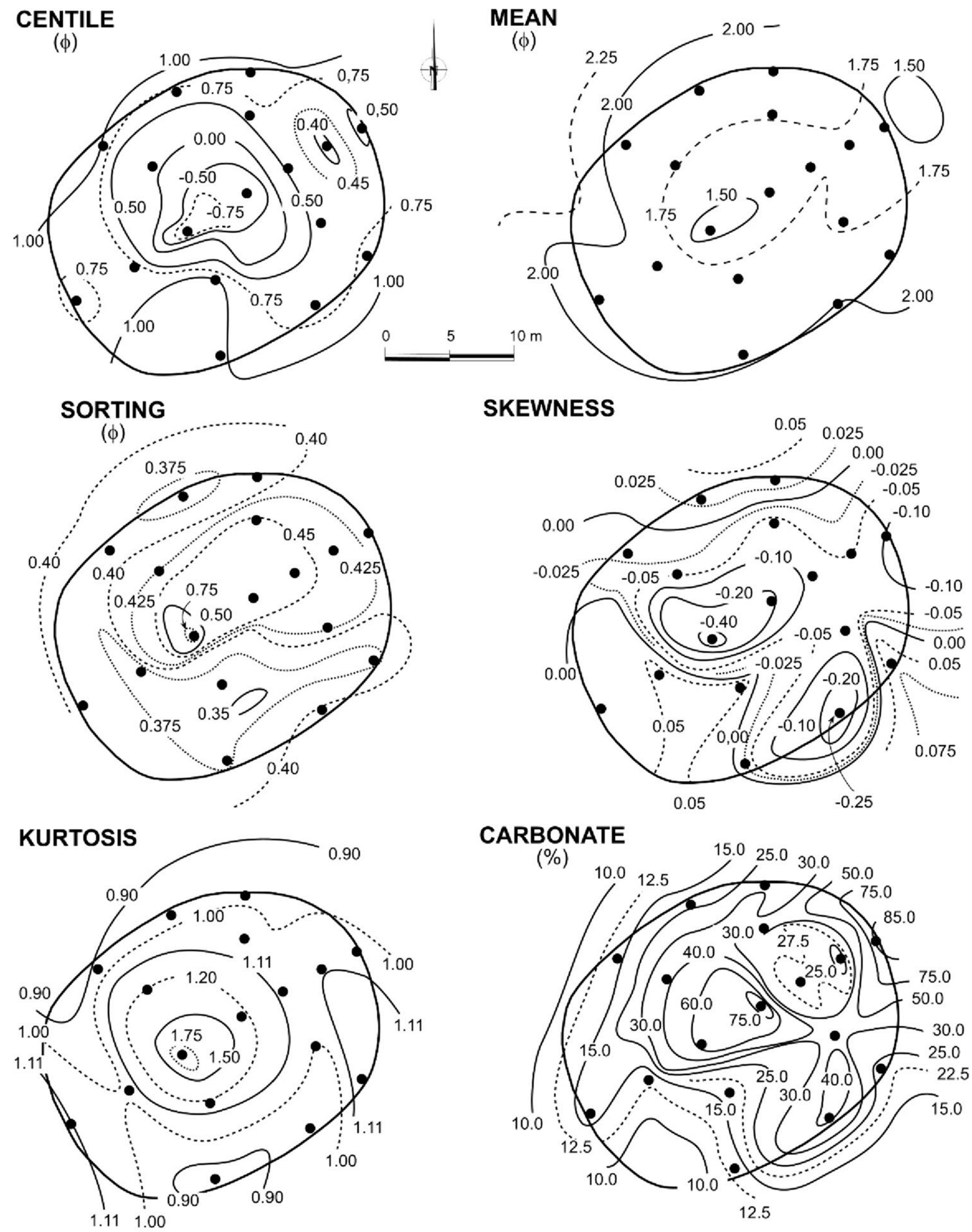

Fig. 7 Trend mapping of grain-size parameters centile and mean, sorting, skewness ans kurtosis, as well as the biogenic carbonate percent in the dune field of saucer blowout in the sandy spit of El Puntal (Somo)

4.3 Sonabia

The studied blowout has an irregular sub-elliptical contour, and slightly contrasted slopes; it is opened on the windward side of an isolated transverse dune in the inner side of the dune field, generated by NW winds (Figs. 3G, 8A–C). The altimetric contrasts are lower than 4 m. It is relatively loose and acquires an elongated shape with the major axis in direction ENE-WSW; within it, two depressions have been over-excavated. The western one is about half the size, whose bottom acquires an NNW-SSE direction. They are separated by a step with a difference less than 0.5 m (Fig. 8B, C). This same type of bowl, but with a wider and longer bottom elongated NNO-SSE, is activated on the eastern side, developing between them a step of 0.25 m in height, depressed towards the W. The sedimentary rim is restricted to the southern edge with the corresponding crest that embraces the over-deepening bottom, and extends somewhat further along the western side (Figs. 3F, 8B, C).

The aeolian sandy sedimentation has been concentrated on the southern edge, most likely by prevailing winds of NW and NE, which would explain the continuation of the southwestern sedimentary ridge that would activate the formation of the two elongated NNW-SSE over-excavation depressions. The angles of inclination of the sedimentary

Table 3 Averages of the grain-size parameters and the biogenic carbonate percents for each particular morphology in the blowout of El Puntal of Somo

	Centile		Mean		Sorting	Skewness	Kurtosis	Carbonates
	(ϕ)	(mm)	(ϕ)	(mm)	(ϕ)			(%)
SW outer side	−0.07	1.95	1.63	0.32	0.51	−0.01	1.00	14.90
NE outer side	0.48	0.72	1.78	0.29	0.20	−0.05	1.04	45.77
Crest	0.83	0.56	1.91	0.27	0.39	0.06	0.94	19.45
SW inner side	0.52	0.70	1.73	0.30	0.46	−0.15	1.94	12.90
NE inner side	0.96	0.51	1.89	0.27	0.38	−0.05	1.09	25.40
Bottom	0.48	0.72	1.73	0.30	0.46	−0.11	1.21	41.42

rim on its windward flank (northern area) are higher, reaching 30°, due to the frontal effect of the mentioned winds (Figs. 3F, 8C).

The sands that make up the main transverse dune and the open blow correspond to fine sands and are very well sorted (Fig. 9). The tendencies of the values of the centil are more or less distributed in concordance with the plant of the two erosive sub-basins, even lengthening in the pointed NNW-SSE direction. They are mostly represented by the coarser sizes (1.55φ), both in these and in part of the sedimentary rim; but a thinner belt is represented by finer sand (1.75φ) on the northern flank, all western and half N of the eastern side (Fig. 9). The values of the mean size follow the same trends with larger grain sizes of (2.25φ) that would also affect the sedimentary rim and a belt of finer ones at the northern end (2.50φ), which envelop part of the northern flanks of the W and E sides.

The aeolian sands of Sonabia (Fig. 9), like those of Frouxeira, are very well sorted (0.20 to 0.35φ), drawing elongated NNW-SSE curves, which reach 0.35φ in both sub-basins, while surpassing to even better values towards the western flank (0.30φ) and optimal in the northeast (0.20φ).

The skewness shows a certain uniformity (Fig. 9), being better in the eastern bottom; values close to 0 or slightly negative are developed in the depression (−0.05 and −0.10), which gradually become more negative towards the N. On the other hand, in the western area, they are very negative, even the most extreme (−0.50). The isolines of the kurtosis also reproduce an adaptation to the bottom with proper isolines of flat curves (0.75), which gradually pass to increasingly sharp curves (1.11) towards the northern flanks (Fig. 9). The biogenic carbonates draw the same tendency, but with less precision; they are maximum in the bottoms of the sub-basins (72.50%), decreasing outwards, both on the strip containing the sedimentary rim (fluctuating values from 62.5 to 72.5%) and more regularly in the north where the minimum is 62.5% (Fig. 9).

Although the data of surface samples are limited in this blowout, they serve to complement those referring to the previous ones of Frouxeira and the Somo Spit (Table 4). The centile is a statistically worse granulometric parameter (higher values), but in many cases it reports better than the mean size, which represents more smooth values. The bottom reaches the maximum average kinetic energy (1.54φ = 0.34 mm), while the crest (1.60φ = 0.33 mm) and the internal sidewall (1.62φ = 0.33 mm) are more uniform with each other.

The sorting is subtly better on the crest (0.32φ), like the windward flank (0.33φ) and the bottom: 0.35φ. The skewness is different, more negative in the crest (−0.30), decreasing in the inner NW flank (−0.19) and in the bottom (−0.15). The kurtosis varies within the platykurtic category, specially in the crest (0.73), followed by the bottom (0.80) and the inner side that tends to mesokurtic (0.85). The biogenic carbonates do not offer contrasts, being maximum in the bottom coinciding with the highest energy (72.76%), followed by the inner NW flank (71.14%) and the crest (70.60%).

5 Discussion

The sandy beaches with sedimentary surpluses represent accumulations capable of supplying that sand fraction to deflation of the wind from sea to land, generating dune fields in the back areas. These are natural systems that protect the associated beach, especially by the action of wave storms (Hobbs, 2012). Therefore, both phenomena are fundamental in the coastal sedimentary balance (Rosati, 2005), interacting closely (Sherman & Bauer, 1993) in terms of its morphodynamic.

Few studies have been carried out on granulometric features in coastal dunes and dune fields, highlighting those of Flor (1986), Alcántara-Carrió (2003) and Martínez Cedrún (2009). In this paper, complementary morphological contributions on saucer blowout types are established, including data from the coastal dune fields of Frouxeira (Flor, 1984), Somo and Sonabia (Flor & Martínez Cedrún, 1991; Martínez Cedrún, 2009).

Blowouts are considered aeolian features consisting of an erosional depression and, in many cases, an associated downwind depositional lobe or apron (Baird et al., 2021; Hesp, 2002; Smyth et al., 2020). In this work it is shown that the simplest ones consist of an erosive or non-sedimentary

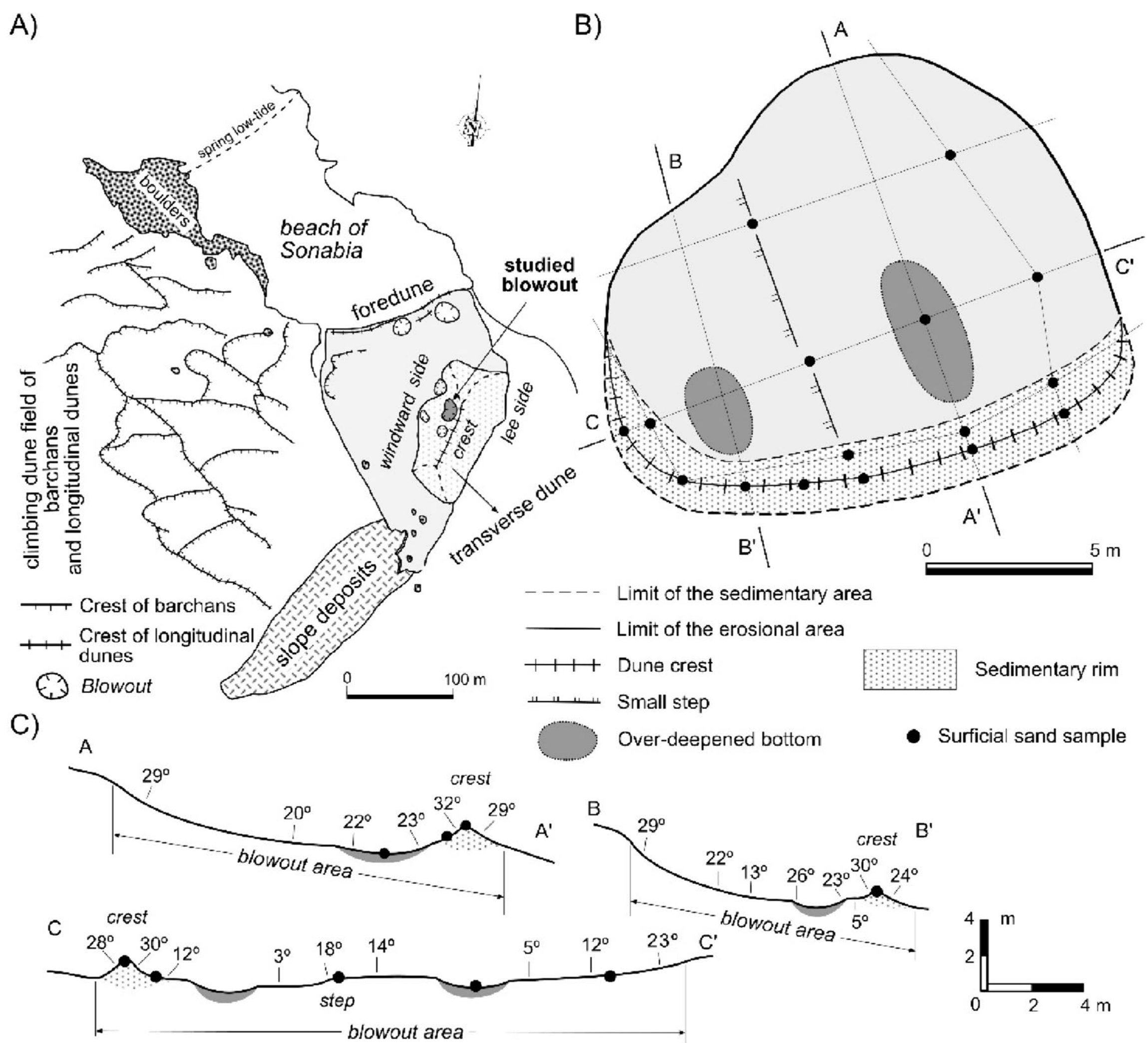

Fig. 8 **A** Location of the studied blowout on the windward side (more exposed to wind) of the internal transverse dune of the Sonabia complex. **B** The two small depressions are separated by a slightly contrasted step, developing a sedimentary rim in the southern area. **C** Several representative transverse profiles have been made, including the position of the surface sandy samples

depression where lag deposits are concentrated and a sedimentary rim that surrounds the entirety or a large part of the dune; it should be noted that no downwind sedimentary lobe has been built. Usually, they are developed on a previous sandy accumulation (Sloss et al., 2012) as it happens, but more probably reworking of old sands and new sedimentation occur as would be the cases of Frouxeira and Somo.

These blowouts belong to varied saucer typologies, all of them being sub-elliptic plant with the major axis oriented in the direction of the dominant wind; the sedimentary rims vary from narrow and incomplete in Sonabia, to almost the whole perimeter in Frouxeira, and fully developed in the blowout of El Puntal of Somo. In Frouxeira, the bottom or deflation basin is very flat, relatively broad and shallow due to the very epidermic position of the water table; that of the spit of El Puntal would represent a shallow blowout that has been re-excavated over the central circle of the deflation basin in what could constitute an evolutionary stage tending to consolidate a bowl-blowout type; and that of Sonabia is double and little deepened.

Gares and Nordstrom (1995) differentiated a set of primary geomorphological features, mainly of erosional origin, such as erosional throat and steep lateral walls adjacent to the throat, including a depositional lobe in the lee side. In a through blowout, open to the adjacent beach, Fraser et al. (1998) distinguished up to 9 morphological elements, some of which are identified in an isolated saucer blow: entrance or throat, sedimentary belt (rim) with the culminating ridge, deflationary floor, avalanche faces, escarpment, sliding blocks, spillove lobes, lateral extensional lobes, etc.

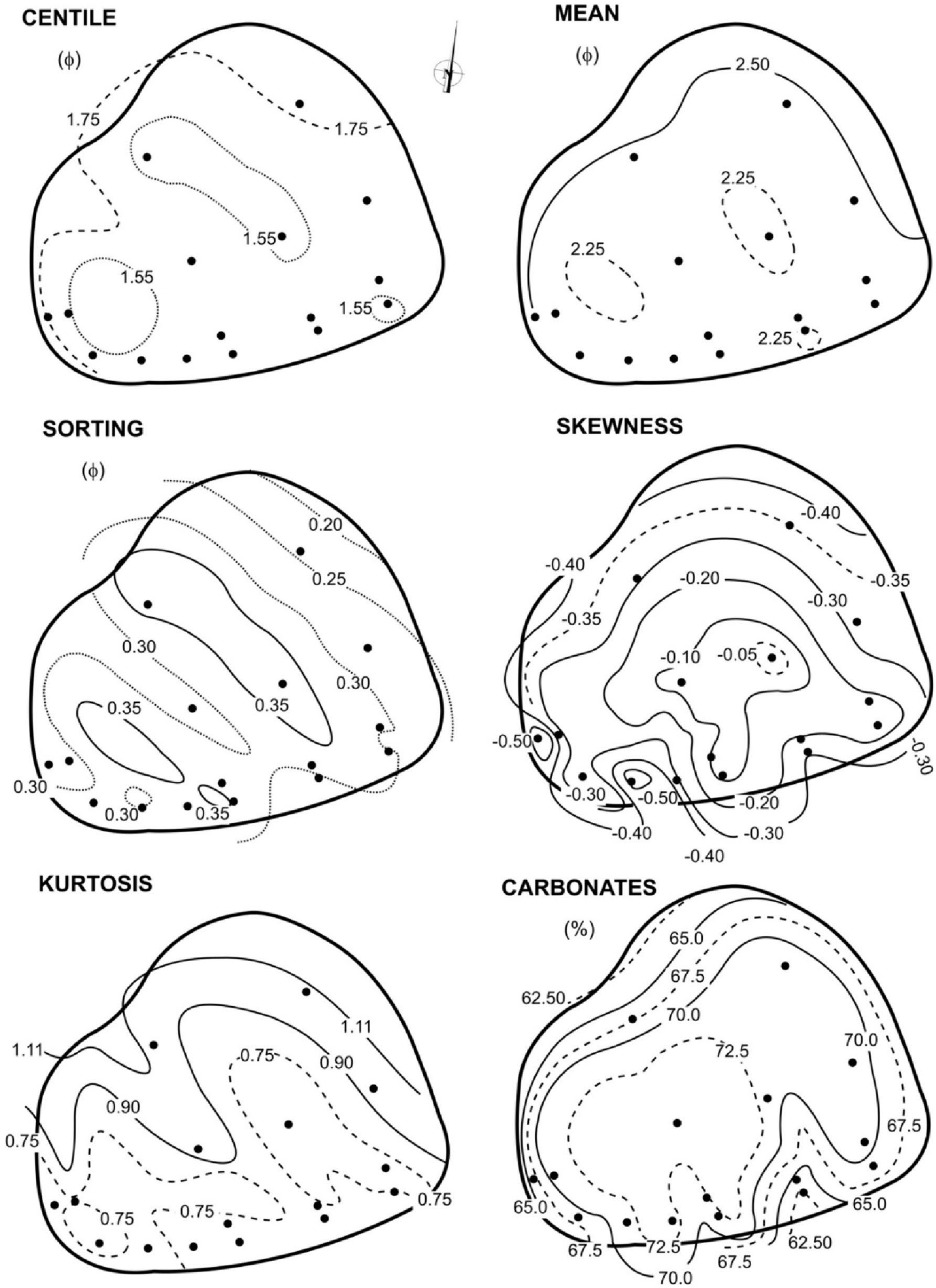

Fig. 9 Trend maps of the grain-size parameters of range (centile) and relation (mean, sorting, skewness and kurtosis), as well as the biogenic carbonate content (%) in the saucer blowout of Sonabia (modified after Flor & Martínez Cedrún, 1991)

Table 4 Averages of grain-size parameters and biogenic carbonate percents for each particular morphology in the blowout of Sonabia

	Centile		Mean		Sorting	Skewness	Kurtosis	Carbonates
	(ϕ)	(mm)	(ϕ)	(mm)	(ϕ)			(%)
Crest	1.60	0.33	2.37	0.19	0.32	−0.30	0.73	70.60
Bottom	1.54	0.34	2.30	0.20	0.35	−0.15	0.80	72.76
NW inner side	1.62	0.33	2.34	0.20	0.33	−0.19	0.85	71.14

Major axis is related to the incoming high magnitude winds (Gares & Nordstrom, 1995), and zones of recirculation of airflow of up to 180° off of the incoming wind direction are recorded (Fraser et al., 1998; Hugenholtz & Wolfe, 2009). Although there is a dependence on the degree of exposure to winds from several directions (Jennings, 1957; Shepherd et al., 1997), this paper proposes a simple conceptual model of flow dynamics for a single prevailing wind direction (Fig. 10) according to several authors (Hesp & Hyde, 1996; Hesp, 2011; Hesp & Walker, 2012; Smyth et al., 2012; Sun et al., 2016; Schwarz et al., 2019; Smyth et al., 2019). It would obviously be the dominant one according to Jungerius and van der Meulen (1989) who found that the blowouts grow in length towards where the wind blows.

Flow dynamics in saucer blowouts is complex as a result of varying wind speeds and direction with flow separation occurring around much of the erosion walls, allowing also complex erosion and deposition (Fig. 10), that occurred in distinct regions within the blowout (Smyth et al., 2019). Saucer blowouts commonly grow in length upwind against the prevailing wind. The flow up trough blowouts is commonly topographically accelerated, and displays marked single and double jets up the deflation basin, corkscrew vortices over the lateral erosional wall crests, and rapid flow deceleration and lateral expansion (Hesp & Hyde, 1996).

Blowouts are sensitive to local winds in the development of their morphometry (Bolles, 2012) and vegetation can play an important role because it represents an important controlling factor, determining if a dune system will become stabilized or activated (Nield & Baas, 2008). Blowing winds, considering the relationship between the direction of the generator wind and the resulting dune geometry (Flor & Flor-Blanco, 2014c), can be established. Thus, the two recorded components by the regional meteorological stations are: NE for Frouxeira (Fig. 2B) and NE in the El Puntal spit (Fig. 2C) and, almost certainly, NW in the case of Sonabia (Fig. 2D), together with less intervention of the NE, of a secondary nature. Onshore winds accelerate through the blowout and they experience rapid flow deceleration, lateral expansion and in some cases flow separation (Fraser et al., 1998). The wind incidence determines the geometry of the hollow (simplified the bottom and sedimentary rim), the peculiarities of its represented geometries and the distribution of the sediment, characterized by its grain-size parameters and mineralogical composition (siliciclastics versus carbonate bioclasts). Blowout patterns typically align with the direction of maximum exposure of wind, so wind pattern compounds morphological development as well (Ritchie, 1972).

Despite the sub-elliptic geometry and the continuity of the ridge, two flanks are identified in some sections, right and left each one with inner and outer sides; it is related to the direction of the dominant wind in its formation and evolution, also applicable to longitudinal dunes, as part of the whole. On the other hand, the windward and leeward flanks, both external and internal, as well as the crest and the deflation bottom have been systematically considered (Fig. 10, Table 5).

A first contribution of studied blows, without a sedimentary lobe downwind, allows morphological sectorizing of each one (Fig. 10), although there is a total continuity of the sedimentary rim around the depression in the case of greater complexity, such as that of El Puntal of Somo, almost complete in Frouxeira and partially in Sonabia (less than half the contour). This picture constitutes a first step to understand the relationship between the air flows and the distribution of the granulometric parameters, carbonate percentages and average slopes.

Anderson and Walker (2006) deduced from well-sorted sands of the beach, fine skewed backshore sands become more poorly sorted and coarse skewed in the blowout due to winnowing of fines. In the blowouts and their morphologic areas, the works are practically nonexistent.

The wind as a selective energy factor can act more effectively on the fine sedimentary fractions of a broad sandy population distribution, endowing it with specific characteristics. So, deflation promotes a deposit of sand dunes somewhat finer than the beach of origin; in addition, they are much better sorted and skewness tend to be more positive (or less negative) and curves (kurtosis) are more acute (Flor et al., 1983, 2022; Flor, 1981b; Friedman, 1967; Giles & Pilkey, 1965; Matias et al., 2005). Finally, the carbonate content is lower in dunes than the associated sandy beach (Flor & Flor-Blanco, 2009; Flor et al., 2022; Flor, 1981a; Martínez Cedrún et al., 2014; Shepard & Young, 1961).

Other studies have focused on trough-shaped blowouts, some about the temporal evolution of sedimentary movements (Smith, 2013). Other results limit the value of this type of granulometric distributions in relation to the transport patterns in this type of blowout (Randolph, 2013). The

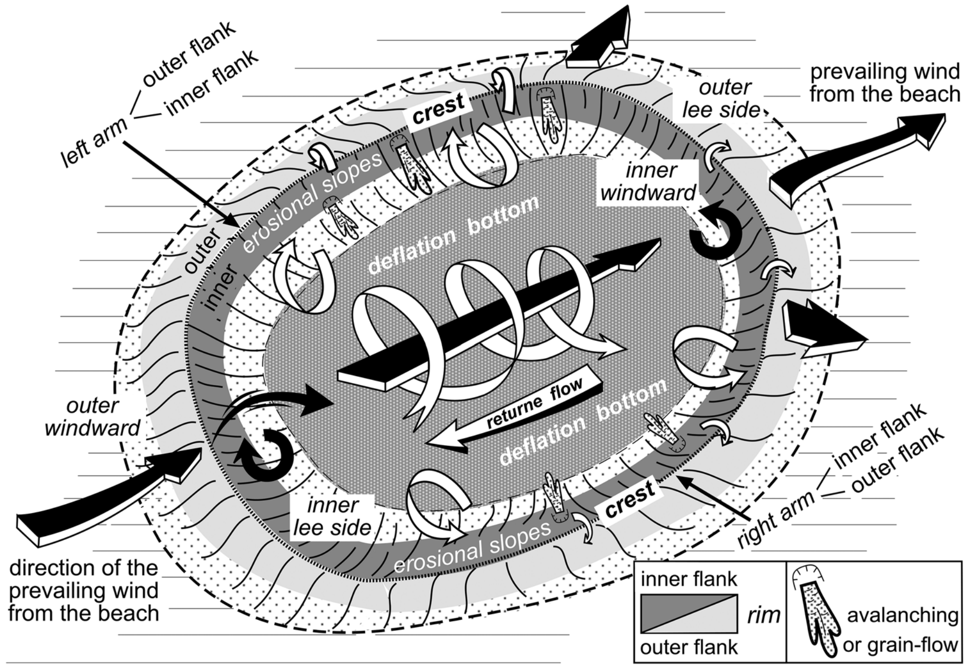

Fig. 10 Simplified conceptual model, based in flow dynamics of a semi-elliptical blowout developing a uniform sedimentary rim and a flat bottom controlled by the water table, detailing the morphological units. The arrows indicate the main sedimentary flows (larger black arrows) and secondary arrows (smaller curved arrows), also considering a simple wind component adapted to the major axis

Table 5 Relative absolute values of the grain-size parameters, biogenic carbonate percents and angles of inclination (slope) of each morphological area: windward and lee sides, crests and bottoms, synthesized from the three studied saucer blowouts

	Mean size	Sorting	Skewness	Kurtosis	Carbonates	Angle of inclination
Outer windward side	Coarse	Good	Very variable	Flat-moderate	Very low	Moderate
Outer leeward side	Coarse	Better	Very variable	Flat-moderate	Maximum	Very high
Crest	Finner	Very good	Very variable	Flat-moderate	Very low	Gentle
Inner windward side	Coarse	Good	Very variable	Very sharp	Minimum	Very high
Inner leeward side	Moderate	Good	Extreme	Moderate sharp	Moderate	High
Bottom	Coarser	Moderate	Very variable	Sharp	Very high	Gentle
Inner right side	Moderate	Moderate	Very variable	Flat	High	Very high
Inner left side	Moderate	Good	Very variable	Moderate-sharp	High	Very high
Outer right side	Finer	Moderate	Very variable	Moderate	Low	High
Outer left side	Finer	Good	Very variable	Sharp	Moderate	Moderate

windward side of the blowout has coarse grains, sorting is very good and coarse at the bottom with worse sortings (Tripaldi, 2001). Grevenhoed et al. (2016) found small differences in grain-size parameters being the main size of medium sands; sand at the crests of saucer blows has a good sorting, are strongly coarse-skewed and curves are mesokurtic; in trough blows, crest are represented by similar average values and the bottom is characterized by a very well sorting, almost symmetrical curves and leptokurtic ones.

Tendency maps of the grain-size parameters and carbonate biogenic percent (versus quartz content) agree to adjust a semicircular or sub-elliptical plant of saucer blowouts (Figs. 5, 7, 9). The main diameter is the best grain-size parameter that reflects the sediment responses (Liu & Zarillo, 1989) to hydrodynamic factors, manifested by their decrease in transport direction (eg Allen, 1970; Bird, 1969). This is particularly true in free and coastal dunes, as foredunes (Arens et al., 2002), including the most frequently estudied desert dunes (Koeshidayatullah et al., 2016). The coarsest fraction of a grain-size population should move near the bed (Shao, 2008), but mean grain-size is not constant with height and, from the grain-size inflection that occurs between 0.05 and 0.15 m above the bottom, there is a coarsening of mean size with elevation (Farrell et al., 2012).

In the saucer blowout of Frouxeira, the absolute values of the grain-size parameters usually show subtle differences, so that very small variations allow to deduce significant dependencies in the cause/effect relationship (aeolian/sedimentation-erosion). Thus, the average values of the main sizes (2.05–2.09φ) are quite regular and other parameters do not show very significant differences, except for the case of the centile. These sands are practically decalcified due to its relative old age during which the carbonate bioclasts have dissolved in the rain and are fixed by vegetation in these climbing dunes of Frouxeira.

Crests of studied blows are represented by comparative finner sands, while the bottoms are the coarsest. The constituent parts of transverse dunes (windward and leeward flanks, and crest) and longitudinal dunes (right and left flanks and crest) show characteristic distributions (Flor, 1981b). In coastal tongue-like dunes, for example, the crests are represented by finer sizes and better sortings, while the bioclastic carbonate percentages are lower than foredunes (Flor, 1986), both representative of transverse and longitudinal coastal dunes, respectively.

In these studied blows, the relative average values are revealing (Table 5). Sands are coarse around the whole rim, as well as in the deflation bottom, except for the inner lee side in which they are moderate, and along the crest where are finer. Only the sorting is better on the windward side of Frouxeira, worsening downwind. In El Puntal of Somo, the largest mean size is housed on the windward side, decreasing to fine once the entire blowout has been overcome, downwind; the isolines of the skewness go from negative to almost symmetrical in the same direction, as well as the sharpness of curves that from mesokurtic-platykurtic ends in flat; finally, carbonate percents are higher in windward side and evolve to lower percentages to leeward side. In Sonabia, the main sizes are also fine in windward side and acquire even finer sizes, the skewness vary from negative to more negative and the kurtosis of the curves from mesokurtic to platykurtic, in all cases at the end of the blowout, downwind.

Although the representative samples are scarce on the right and left sides, with respect to the dominant wind flow, some deductions can be summarized, except the skewnees (Table 5). Main sizes are moderate in the inner right and left sides and finer in the outer flanks, gradually moving to the bottom of larger sizes (more energetic areas). Sorting is moderate in the inner and outer rigth sides, but good in the others opposed sides. Some major variations have been obtained for the kurtosis, generally with flat and moderate curves in the inner sides and sharp curves in the outer left side. Carbonate percents are high in inner flanks (coarse sands) and vary from low to moderate in outer flanks. Inner flanks develop very high slopes, that decrease to the outer right side and they are miminum in the outer left side.

The external sides are characterized by finer mean sizes, moderate sorting, sharp curves, moderate carbonates and slopes are of lower; the inner right flanks have comparatively lower slopes than those of the opposite inner right flank, where the greater energy determines a greater slope if it is an angle of repose for dry dune sand, usually 34° (Fryberger & Schenk, 1981) or 45° for wet sand, and particle size, complex geometric particle shapes and humidity contribute to producing steeper granular surfaces (Al-Hashemi & Al-Amoudi, 2018). Erosional walls can reach slopes of 65° due to strong erosive processes, as in the blowout of Somo (Fig. 6B).

It is practically universal that the flanks of the internal walls and more specifically the upper parts develop slopes greater than 30°, that are indicative of the preponderance of erosive processes in these cases; the outer flanks reduce the angle of inclination with respect to the internal ones. Outer windward and outer lee sides adquire moderate and very high angles of inclination (Table 5) as if they were a single transverse dune without an intermediate bottom. Inner windward slope is maximum due to the frontal impact of the wind developing strong airflows, capable of eroding with retrait the dune side (Fig. 10).

The deflation bottom acquires flat or somewhat convex surfaces downwards, best represented in Frouxeira (Fig. 4C), which respond to strong winds which over-deepen the enclosures, and where there are concentrated lag deposits, characterized by coarser grain sizes, moderate sortings, sharp curves and high bioclastic carbonate percents. An over-excavation of the deflation bottom can trigger the formation of a new inscribed hollow with slopes greater than 60°, which can indicate an ongoing evolution in the Somo blowout (Fig. 6B), represented by a deepening, to a bol-type blowout from a shallow one (Thomas, 2004).

6 Conclusions

Studied saucer blowouts, with no downwind sedimentary lobe, of coastal dunes in the NW Spain are part of a sequence of dune typologies that incorporate a simple sedimentary rim, from partial in Sonabia to full developed in Frouxeira and Somo, and an erosive depression (deflation bottom) that in Frouxeira is controlled by the phreatic water level. One of them is represented by a double over-excavation hollow in two sub-basins (Sonabia) or a central over-deepened area trending to the construction of a bowl (Somo).

The dominant direction of the wind is established: NE in Frouxeira and El Puntal of Somo and NW in Sonabia, directly related to the major axis, that generates the erosive and sedimentary depression. It is proposed to divide these blows into different morphological parts, despite the total morphological continuity of the ridge: crest and deflation bottom, right (inner and outer) and left (outer and inner) flanks, elongated according to the direction of the wind, downwind, outer windward and inner lee ward flanks, inner windward and outer lee ward flanks.

The sedimentological characterization of each of them is the result of the wind dynamics on the dune set in the depositional process, better represented for the average size (higher in the outer windward and deflation bottom and minimum in the crest); the sorting is better in the outer lee side and moderate on the bottom; the skewness show no contrasts of interest being only extreme in the inner lee side; less sharp curves are represented on the windward and leeward flanks and crest, and are leptokurtic on the leeward side; bioclastic carbonate percents are maximum on the outer lee ward side, followed by the bottom and are minimum on the inner windward side. It is complemented by the average slopes in the flanks: very high in the outer leeward and internal windward, moderate in the outer windward and flat in the crest and deflation bottom.

This limitation of data suggests that detailed studies should be undertaken in the future, including more meticulous topographic surveys with terrestrial laser scanner (TLS) techniques, and incorporating new typologies of blowouts, in order to establish comparable patterns in morphological and sedimentary distributions, the most interesting features studied in this paper.

Casquetes del tipo "soucer blowout" en los campos dunares de la costa del NO de España, Península Ibérica

Resumen

Palabras clave .

Funding Open Access funding provided thanks to the CRUE-CSIC agreement with Springer Nature. The authors have not received any funding to carry out this work.

Declarations

Conflict of interest The authors declare that they have no conflict of interest.

References

Abhar, K. C., Walker, I. J., Hesp, P. A., & Gares, P. A. (2015). Spatial-temporal evolution of aeolian blowout dunes at Cape Cod. *Geomorphology, 236*, 148–162. https://doi.org/10.1016/j.geomorph.2015.02.015

Alcántara-Carrió, J. (2003). *Dinámica sedimentaria eólica en el istmo de Jandía (Fuerteventura). Modelización y cuantificación del transporte*. Servicio de Publicaciones del Excmo. Cabildo Insular de Gran Canaria, Spain. Ph.D. thesis, 288 pp.

Al-Hashemi, H. M. B., & Al-Amoudi, O. S. B. (2018). A review on the angle of repose of granular materials. *Powder Technology, 330*, 397–417. https://doi.org/10.1016/j.powtec.2018.02.003

Allen, J. R. L. (1970). A quantitative model of grain size and sedimentary structures in lateral deposits. *Geological Journal, 7*, 129–146. https://doi.org/10.1002/gj.3350070108

Anderson, J.L, Walker, I.J. (2006). Airflow and sand transport variations within a backshore-parabolic dune plain complex: NE grahamisland, british columbia, canada. *Geomorphology*, *77*(1-2), 17–34. https://doi.org/10.1016/j.geomorph.2005.12.008

Arens, S. M., van Boxel, J. H., & Abuodha, J. O. Z. (2002). Changes in grain size of sand in transport over a foredune. *Earth Surface Processes Landforms, 27*, 1163–1175. https://doi.org/10.1002/esp.418

Baird, T. R., Bristow, C. S., Luo, W., Du, E., Bryant, R. G., Mitchell, T. M., & Wermeesch, P. (2021). Blowout morphometrics and mass balances. *Frontiers Earth Science, 9*, 669440. https://doi.org/10.3389/feart.2021.669440

Barchyn, T. E., & Hugenholtz, C. H. (2012). Predicting vegetation-stabilized dune field morphology. *Geophysical Research Letters, 39*, L17403. https://doi.org/10.1029/2012GL052905

Bird, E. C. F. (1969). *Coasts: An introduction to systematic geomorphology* (p. 246). The MIT Press.

Blott, S. J., & Pye, K. (2001). GRADISTAT: A grain size distribution and statistics package for the analysis of unconsolidated sediments. *Earth Surface Processes Landforms, 26*, 1237–1248. https://doi.org/10.1002/esp.261

Bolles, K. C. (2012). *Post-emplacement coastal dune blowoutdevelopment and re-colonization*. M.Sc. thesis. Environmental Mapping. UCL Department of Geography. University College London, 50 pp.

Carter, R. W. G., Hesp, P. A., & Nordstrom, K. F. (1990). Erosional landforms in coastal dunes. In K. F. Nordstrom, N. Psuty, & B. Carter (Eds.), *Coastal dunes, form and process* (pp. 217–250). West Sussex: Wiley.

Cooper, W. S. (1958). *Coastal sand dunes of Oregon and Washington* (Vol. 72, p. 169). Geological Society American Memoir.

Cooper, W. S. (1967). *Coastal dunes of California* (Vol. 104, p. 131). Geological Society American Memoir.

Davidson-Arnott, R., Bauer, B., & Houser, C. (2019). *Introduction to coastal processes and geomorphology* (2nd ed.). Cambridge University Press.

de Sanjosé, J. J., Gómez, M., Serrano, E., Sánchez, E., Flor-Blanco, G., & Ferreira Sousa Cruz, P. M. (2017). Análisis de temporales (1985–2016) y cambios de la línea de costa (1875–2016) en la playa de "El Puntal-Somo-Las Quebrantas-Loredo" (Cantabria). *Geo-Temas, 17*, 51–54.

de Sanjosé, J. J., Gómez-Lende, M., Sánchez-Fernández, M., & Serrano-Cañadas, E. (2018). Monitoring retreat of coastal sandy systems using geomatics techniques: Somo Beach (Cantabrian Coast, Spain), 1875–2017. *Remote Sensing, 10*, 1500. https://doi.org/10.3390/rs10091500

de Sanjosé, J. J., Gómez-Lende, M., Sánchez-Fernández, M., & Serrano-Cañadas, E. (2021). Geomatics techniques for monitoring the retreat of coastal sandy systems: Somo Beach (Cantabrian coast, Spain, 1875–2017). In G. Y. Sheu (Ed.), *Newest updates in physical science research* (Vol. 8, pp. 30–50). Book Publisher International. https://doi.org/10.9734/bpi/nupsr/v8/1775F

Depuydt F. (1972). *De Belgische strand- en duinformaties in het kader van de geomorfologie der zuidoostelijke Noordzeekust*. Koninklijke Akademie voor Wetenschappen, Letteren en Schone Kunsten van België. Klasse der Wetenschappen, Jaargang 34 (122), Brussel, 34 (122), 228 pp.

Elorza, J., & Higuera-Ruiz, R. (2015). Morfologías escalonadas de erosión eólica y disolución química sobre las calizas Urgonianas en la playa de Valdearenas (Sonabia, Cantabria). *Revista De La Sociedad Geológica De España, 28*(1), 25–39.

Farrell, E. J., Sherman, D. J., Ellis, J. T., & Li, B. (2012). Vertical distribution of grain size for wind blown sand. *Aeolian Research, 7*, 51–61. https://doi.org/10.1016/j.aeolia.2012.03.003

Felicísimo Pérez, A. M. (1992). El clima de Asturias. In *Geografía de Asturias* (Vol. 2, pp. 17–32). Ed. Prensa Asturiana, S.A. Oviedo, Asturias.

Fernández-Valdés, J.M., Flor, G. & Viña, C. (1994). The bioclastic component of the inner shelf surficial sediments in the Asturian central area (NW Spain, Bay of Biscay). In *GAIA, Revista de Geociências* (Vol. 8, pp. 135–138). University of Lisboa.

Feuillée, P., & Rat, P. (1971). Structures et paléogéographies pyrénéo-cantabriques. In J. Debyser, X. Le Pichon, & L. Montadert (Eds.), *Colloque de l'Histoire du Golfe de Gascogne* (Vol. 2, pp. 1–45). Technip.

Fillon, C., Pedreira, D., van der Beek, P. A., Huismans, R. S., Barbero, L., & Pulgar, J. A. (2016). Alpine exhumation of the central Cantabrian Mountains, Northwest Spain. *Tectonics, 35*, 339–356. https://doi.org/10.1002/2015TC004050

Flor, G. (1981a). Los parámetros texturales en las playas y dunas arenosas del borde occidental del Cabo Peñas (Xagó y Verdicio, Asturias). *Boletín De La Real Sociedad España De Historia Natural (geología), 79*, 89–102.

Flor, G. (1981b). Las dunas eólicas costeras de la playa de Xagó (Asturias). *Trabajos De Geología, 11*, 61–71.

Flor, G. (1984). Estudio sedimentológico y morfológico de una duna costera "blowout" (Cabo Frouxeira, La Coruña). *Trabajos De Geología, 13*, 161–174.

Flor, G. (1986). Sedimentología de una duna lingüiforme en la playa de Xagó (Asturias). In *Proceedings IX Congreso Nacional de Sedimentología* (pp. 317–328). Servicio de Publicaciones, Universidad de Salamanca I.

Flor, G. (1992). Tipología, catalogación y procesos erosión/sedimentación de los campos dunares eólicos de Galicia (NO de España). *Thalassas, 10*, 9–39.

Flor, G. (2004). Modelos evolutivos de los grandes campos dunares de Asturias El factor antrópico. In R. Blanco Chao, J. López Bedoya, & A. Pérez Alberti (Eds.), *Procesos geomorfológicos y evolución costera. Proceedings II Reunión de Geomorfología Litoral* (pp. 167–181). Servicio de Publicaciones de la Universidad de Santiago de Compostela.

Flor-Blanco, G., & Flor, G. (2019). Cantabrian estuaries. In J. A. Morales (Ed.), *The Spanish coastal systems, dynamic processes, sediments and management* (pp. 415–436). Springer. https://doi.org/10.1007/978-3-319-93169-2_18

Flor, G., & Flor-Blanco, G. (2009). Sedimentología de los depósitos arenosos superficiales de la playa de Vega (Concejo de Ribadesella, Asturias). *Revista De La Sociedad Geológica De España, 22*(1–2), 105–121.

Flor, G., & Flor-Blanco, G. (2014a). Raised beaches in the Cantabrian coast. In F. Gutiérrez & M. Gutiérrez (Eds.), *Landscapes and landforms of Spain. World geomorphological landscapes* (pp. 239–248). Springer Science+Business Media. https://doi.org/10.1007/978-94-017-8628-7_20

Flor, G., & Flor-Blanco, G. (2014b). Subsistemas estuarinos de la bahía de Santander (Cantabria, Norte de España). In S. Schnabel & A. Gómez (Eds.), *Proceedings XIII Reunión Nacional de Geomorfología* (pp. 568–571). SEG-Universidad de Extremadura.

Flor, G., & Flor-Blanco, G. (2014c). Componentes de viento generadores de morfologías y campos de dunas costeras en Asturias (NO de España). *Cuaternario y Geomorfología, 28*(3–4), 47–68.

Flor, G., & Flor-Blanco, G. (2016). Transformaciones morfosedimentarias de la bahía estuarina de Santander relacionadas con el desarrollo portuario y urbano (Cantabria, NO de España). *Trabajos De Geología, 35*, 139–162. https://doi.org/10.17811/tdg.36.2016.139-162

Flor, G., Flor-Blanco, G., Martínez Cedrún, P., Flores-Soriano, C., & Borghero, C. (2019). Aeolian dune fields in the coasts of Asturias and Cantabria (Spain, NW Iberian Peninsula). In J. A. Morales (Ed.), *The Spanish coastal systems, dynamic processes, sediments and management* (pp. 585–609). Springer. https://doi.org/10.1007/978-3-319-93169-2_25

Flor, G., Flor-Blanco, G., & Rey Ruanova, M. (2022). Transferencias arenosas transversales y longitudinales entre playas apoyadas y dunas asociadas en la costa de Asturias (NO de la península Ibérica). *Revista De La Sociedad Geológica De España, 35*(1), 15–35. https://doi.org/10.55407/rsge.94880

Flor, G., Llera, E. M., & Ortea, J. A. (1982). Los carbonatos biogénicos de los sedimentos de las playas arenosas de Asturias y Cantabria: su origen y significado dinámico. In *Cuaderno del Crinas*, 2, 77 pp. Centro de Investigaciones Acuáticas. Consejo de Gobierno del Principado de Asturias.

Flor, G., Marquínez, J., & O'Neil, A. C. (1983). El complejo de dunas eólicas de la playa de Frouxeira (Meirás-Valdoviño, La Coruña). *Cadernos Laboratorio Xeolóxico Laxe, 6*, 155–187.

Flor, G., & Martínez Cedrún, P. (1991). Características morfológicas y sedimentológicas de las dunas eólicas de Sonabia (zona oriental de Cantabria, NO de España). *Estudios Geológicos, 47*, 317–337. https://doi.org/10.3989/egeol.91475-6427

Folk, R. L., & Ward, W. C. (1957). Brazos River bar: a study in the significance of grain size parameters. *Journal of Sedimentary Petrology, 27*, 3–26. https://doi.org/10.1306/74D70646-2B21-11D7-8648000102C1865D

Fraser, G. S., Bennett, S. W., Olyphant, G. A., Bauch, N. J., Ferguson, V., Gellachs, G. A., Millard, C. L., Mueller, B., O'Malley, P. J., Way, J. N., & Woodfield, M. C. (1998). Windflow circulation patterns in a coastal dune blowout, South Coast of Lake Michigan. *Journal of Coastal Research, 14*(2), 451–460.

Friedman, G. M. (1967). Dynamic processes and statistical parameters compared for size frequency distribution of beach and river sands. *Journal of Sedimentary Petrology, 37*, 327–354.

Fryberger, S. G., & Schenk, C. (1981). Wind sedimentation tunnel experiments on the origin of aeolian strata. *Sedimentology, 28*, 805–821. https://doi.org/10.1111/j.1365-3091.1981.tb01944.x

Gao, S., & Collins, M. B. (1992). Net sediment transport inferred from grain size trends, based upon definition of "transport vectors." *Sedimentary Geology, 80*, 47–60. https://doi.org/10.1016/0037-0738(94)90023-X

García Couto, M. Á. (2011). *Iberian Climate Atlas. Air temperature and precipitation (1971–2000)* (p. 79). Agencia Estatal de Meteorología (AEMET).

Gares, P. A., & Nordstrom, K. F. (1995). A cyclic model of foredune blowout evolution for a leeward coast: Island Beach, New Jersey. *Annals Association American Geographers, 85*, 1–20.

Gares, P. A., & Pease, P. (2014). Influence of topography on wind speed over a coastal dune and blowout system, Jockey's Ridge, NC, USA. *Earth Surface Processes Landforms, 40*(7), 853–863. https://doi.org/10.1002/esp.3670

Giles, R. T., & Pilkey, O. H. (1965). Atlantic beach and dune sediments of the southern United States. *Journal of Sedimentary Research, 35*, 900–910. https://doi.org/10.1306/74D7139D-2B21-11D7-8648000102C1865D

Glenn, M. (1979). Glossary. A study of global sand seas. In E.D. McKee (Ed.), *US Geological Survey professional paper* (Vol. 1052, pp. 399–407).

González-Villanueva, R., Costas, S., Duarte, H., Pérez-Arlucea, M., & Alejo, I. (2011). Blowout evolution in a coastal dune: Using GPR, aerial imagery and core records. *Journal of Coastal Research, SI, 64*, 278–282.

González-Villanueva, R., Costas, S., Pérez-Arlucea, M., Jerez, S., & Trigo, R. M. (2013). Impact of atmospheric circulation patterns on coastal dune dynamics, NW Spain. *Geomorphology, 185*, 96–109. https://doi.org/10.1016/j.geomorph.2012.12.019

Grevenhoed, L. G., DeGraaf, S., Leisman, H. P., McNamara, M. & Sukaria, S. (2016). Interactions between sequential blowouts, their features, and sand transport. *FYRES: Dunes Research Report#22* (pp 16). Department of Geology, Geography and Environmental Studies Calvin College Grand Rapids, Michigan.

Hansen, E., de Vries-Zimmerman, S., van Dijk, D., & Yurk, B. (2009). Pattern of wind flow and aeolian deposition on a parabolic dune on the south-eastern shore of Lake Michigan. *Geomorphology, 105*, 147–157. https://doi.org/10.1016/j.geomorph.2007.12.012

Hesp, P. A. (1999). The beach backshore and beyond. In A. D. Short (Ed.), *Handbook of beach shoreface morphodynamics* (pp. 145–169). Wiley.

Hesp, P. A. (2002). Foredunes and blowouts: Initiation, geomorphology and dynamics. *Geomorphology, 48*, 245–268. https://doi.org/10.1016/S0169-555X(02)00184-8

Hesp, P. A. (2011). Dune Coasts. In E. Wolanski & D. S. McLusky (Eds.), *Treatise on estuarine and coastal science 3* (pp. 193–221). Academic Press. https://doi.org/10.1016/B978-0-12-374711-2.00310-7

Hesp, P. A., Hilton, M., & Konlecher, T. (2017). Flow and sediment transport dynamics in a slot and cauldron blowout and over a foredune, Mason Bay, Stewart Island (Rakiura), N.Z. *Geomorphology, 295*, 598–610. https://doi.org/10.1016/j.geomorph.2017.08.024

Hesp, P. A., & Hyde, R. (1996). Flow dynamics and geomorphology of a trough blowout. *Sedimentology, 43*, 505–525. https://doi.org/10.1046/j.1365-3091.1996.d01-22.x

Hesp, P. A., & Pringle, A. (2001). Wind flow and topographic steering within a trough blowout. *Journal of Coastal Research, SI, 34*, 597–601.

Hesp, P. A., Smyth, T. A. G., Walker, I. J., Gares, P. A., & Wasklewisz, T. (2016). Flow within a trough blowout at Cape Cod. *Journal of Coastal Research, 75*, 288–292. https://doi.org/10.2112/SI75-058.1

Hesp, P. A., & Thom, B. G. (1990). Geomorphology and evolution of active transgressive dunefields. In K. F. Nordstrom, N. P. Psuty, & R. W. G. Carter (Eds.), *Coastal dunes: Form and process* (pp. 253–288). Wiley.

Hesp, P. A., & Walker, I. J. (2012). Three-dimensional æolian dynamics within a bowl blowout during offshore winds: Greenwich Dunes, Prince Edward Island, Canada. *Aeolian Research, 3*(4), 389–399. https://doi.org/10.1016/j.aeolia.2011.09.002

Hobbs, C. H. (2012). *The beach book* (p. 195). Columbia University Press.

Hugenholtz, C. H., & Wolfe, S. A. (2006). Morphodynamics and climate controls of two aeolian blowouts on the northern Great Plains, Canada. *Earth Surface Processes Landforms, 31*(12), 1540–1557. https://doi.org/10.1002/esp.1367

Hugenholtz, Ch. H., & Wolfe, S. A. (2009). Form-flow interactions of an aeolian saucer blowout. *Earth Surface Processes Landforms, 34*(7), 919–928. https://doi.org/10.1002/esp.1776

Jennings, J. N. (1957). On the orientation of parabolic or U-dunes. *Geographical Journal, 123*, 473–480.

Jungerius, P. D., & van der Meulen, F. (1989). The development of dune blowouts, as measured with erosion pins and sequential air photos. *CATENA, 16*, 369–376. https://doi.org/10.1016/0341-8162(89)90021-0

Jungerius, P. D., Verheggen, A. J. T., & Wiggers, A. J. (1981). The development of blowouts in "the blink", a coastal dune area near Noordwijkerhout, the Netherlands. *Earth Surface Proceedings Landforms, 6*, 375–396. https://doi.org/10.1002/esp.3290060316

Koeshidayatullah, A., Chan, S. A., Al-Ghamdi, M., Akif, T., & Al-Ramadan, K. (2016). Discrimination of inland and coastal dunes in Eastern Saudi Arabi desert system: An approach from particle size and textural parameter variations. *Journal of African Earth Science, 117*, 102–113. https://doi.org/10.1016/j.jafrearsci.2016.2016.01.003

Kolm, K. E. (1982). Predicting the surface wind characteristics of southern Wyoming from remote sensing and aeolian geomorphology. In R. W. Marrs & K. E. Kolm (Eds.), *Interpretation of windflow characteristics from eolian landforms* (Vol. 192, pp. 25–54). Geological Society America Special Paper.

Lavín, A., Valdés, L., Sánchez, F., Abaunza, P., Forest, A., Boucher, J., Lazure, P., & Jegou, A.-M. (2004). The Bay of Biscay: The encountering of the ocean and the shelf (18b, E). *The Sea, 14*(24), 933–1001.

Liu, J. T., & Zarillo, G. A. (1989). Distribution of grain sizes across a transgressive shoreface. *Marine Geology, 87*, 121–136. https://doi.org/10.1016/0025-3227(89)90057-1

Lorente-Plazas, R., Montávez, J. P., Jimenez, P. A., Jerez, S., Gómez-Navarro, J. J., García-Valero, J. A., & Jiménez-Guerrero, P. (2015). Characterization of surface winds over the Iberian Peninsula. *International Journal Climatology, 35*, 1007–1026. https://doi.org/10.1002/joc.4034

Losada, M. A., Medina, R., Vidal, C., & Roldán, J. A. (1991). Historical evolution and morphological analysis of "El Puntal" spit, Santander (Spain). *Journal of Coastal Reseaarch, 7*(3), 711–722.

Martínez Cedrún, P. (2009). *Caracterización morfológica y sedimentología de los campos dunares costeros de Cantabria. Evolución ambiental*. Ph.D. Thesis (unpublished). Department of Geology. University of Oviedo, 819 pp.

Martínez Cedrún, P., & Flor, G. (2008). Rasgos morfológicos y sedimentarios del campo dunar de Liencres (Cantabria). In J. Benavente & F. J. Gracia-Prieto (Eds.), *Trabajos de Geomorfología en España, 2006–2008. Proceedings of the X Reunión Nacional de Geomorfología* (pp. 275–278). University of Cádiz.

Martínez Cedrún, P., Flor, G., Flor-Blanco, G., & Maroto González, G. (2014). Relaciones texturales y composición mineralógica de los sistemas de playa/dunas en una costa rocosa: Caso de Cantabria (NO de España). *Revista De La Sociedad Geológica De España, 27*(2), 13–27.

Matias, A., Ferreira, Ó., Mendes, I., Dias, J. A., & Vila-Concejo, A. (2005). Artificial construction of dunes in the south of Portugal. *Journal of Coastal Research, 21*, 472–481.

McKenna, W. (2007). *An evolutionary model of parabolic dune development: blowout to mature parabolic, Padre Island National Seashore, Texas*. LSU Master's Theses. 4153. Department of Geography and Anthropology. University of Hawai, 134 pp. http://digitalcommons.lsu.edu/gradschool_theses/4153

McLaren, P., & Bowles, D. (1985). The effects of sediment transport on grain size distributions. *Journal of Sedimentart Petrology, 55*, 457–470. https://doi.org/10.1306/212F86FC-2B24-11D7-8648000102C1865D

Mir-Gual, M., Pons, G. X., Martín-Prieto, J. Á., Gelabert, B., & Rodríguez-Perea, A. (2017). Dinámica eólica y sedimentaria en el sistema dunar de Cala Tirant (costa N de Menorca). In L. Gómez-Pujol & G. X. Pons (Eds.), *Geomorfología litoral de Menorca: dinámica, evolución y prácticas de gestión. Monografía Societat História Natural Balears* (Vol. 25, pp. 263–281). Palma de Mallorca.

Mir-Gual, M., Pons, G. X., Martín-Prieto, J. Á., Roig-Munar, F. X., & Rodríguez-Perea, A. (2013). Geomorphological and ecological features of blowouts in a western Mediterranean coastal dune complex: A case study of the Es Comú de Muro beach-dune system on the island of Mallorca, Spain. *Geo-Marine Letters, 33*(2–3), 129–141. https://doi.org/10.1007/s00367-012-0298-7

Nield, J. M., & Baas, A. C. W. (2008). The influence of different environmental and climatic conditions on vegetated Aeolian dune landscape development and response. *Global Planetary Change, 64*, 76–92. https://doi.org/10.1016/j.gloplacha.2008.10.002

Pérez Alberti, A., & Vázquez Paz, M. (2011). Caracterización y dinámica de sistemas costeros de Galicia. In F. J. Gracia & E. Sanjaume (Eds.), *Las Dunas en España* (pp. 161–185). Sociedad Española de Geomorfología.

Pérez-Alberti, A., Pires, A., Freitas, L., & Chaminé, H. (2013). Shoreline change mapping along thecoast of Galicia, Spain. *Marine Engineering, 166*(MA3), 125–144. https://doi.org/10.1680/maen.2012.23

Pinazo Ojer, J.M. (2010). *Condiciones climáticas exteriores de proyecto. Guía técnica*. Ahorro y eficiencia energética en climatización 12. IDAE. 123 pp. https://www.idae.es/sites/default/files/documentos/publicaciones_idae/documentos_12_guia_tecnica_condiciones_climaticas_exteriores_de_proyecto_e4e5b769.pdf

Pye, K., & Tsoar, H. (2009). Vegetated dunes. In K. F. Pye, H. Tsoar, & H. (Eds.), *Aeolian sands and sand dunes* (pp. 224–244). Springer. https://doi.org/10.1007/978-3-540-85910-9

Randolph, J.M. (2013). *Evaluating aeolian sand transport vectors in dune blowouts*. Undergraduate Research Scholar Thesis. Texas A&M University. 28 pp. http://hdl.handle.net/1969.1/154872

Ritchie, W. (1972). The evolution of coastal sand dunes. *Scottish Geographical Magazine, 88*(1), 19–35. https://doi.org/10.1080/00369227208736205

Rosati, J. D. (2005). Concepts in sediment budgets. *Journal of Coastal Research, 21*(2), 307–322. https://doi.org/10.2112/02-475A.1

Roy, P. S., & Thom, B. G. (1981). Late Quaternary marine deposition in New South Wales and southern Queensland: An evolutionary model. *Journal of Geological Society Australia, 28*, 471–489. https://doi.org/10.1080/00167618108729182

Schwarz, C., Brinkkemper, J., & Ruessink, G. (2019). Feedbacks between biotic and abiotic processes governing the development of foredune blowouts: A review. *Journal of Marine Science Engineering, 7*, 2. https://doi.org/10.3390/jmse7010002

Shao, Y. (2008). *Physics and modeling of Wind Erosion. Atmospheric and Oceanographic Sciences Library* (Vol. 37, 2 ed.). Springer, 393 pp.

Shepard, F. F., & Young, R. (1961). Distinguishing between beach and dune sands. *Journal of Sedimentary Petrology, 3*(12), 196–214. https://doi.org/10.1306/74D70B37-2B21-11D7-8648000102C1865D

Shepherd, M. J., McFadgen, B. G., Betts, H. D., & Sutton, D. G. (1997). *Formation, landforms and palaeoenvironment of Matakana Island, Bay of Plenty, and implications for archaeology. Science and Research Series 102* (p. 100). Department of Conservation.

Sherman, D. J., & Bauer, B. O. (1993). Dynamics of beach-dune systems. *Progress Physical Geography, 17*(4), 413–447. https://doi.org/10.1177/030913339301700402

Sloss, C. R., Shepherd, M., & Hesp, P. (2012). Coastal Dunes: Geomorphology. *Natural Education Knowledge, 3*(10), 2.

Smith, A., Gares, P. A., Wasklewicz, T., Hesp, P. A., & Walker, I. J. (2017). Three years of morphologic changes at a bowl blowout, Cape Cod, USA. *Geomorphology, 295*, 452–466. https://doi.org/10.1016/j.geomorph.2017.07.012

Smith, A.B. (2013). *Geomorphology of dune blowouts, Cape Cod National Seashore, MA*. Master's Thesis. Department of Geography. East Carolina University, 90 pp. http://hdl.handle.net/10342/4317

Smith, H. T. U. (1960). *Physiography and photo interpretation of coastal sand dunes* (p. 60). Massachusetts University Amherst.

Smyth, T., Thorpe, E., & Rooney, P. (2020). Blowout evolution between 1999 and 2015 in Ainsdale Sand Dunes National Nature Reserve, England. *North West Geography, 20*(1), 13.

Smyth, T. A. G., Hesp, P. A., Walker, I. J., Wasklewicz, T., Gares, P. A., & Smith, A. B. (2019). Topographic change and numerically modelled near surface wind flow in a bowl blowout. *Earth Surface Processes Landforms, 44*(10), 1988–1999. https://doi.org/10.1002/esp.4625

Smyth, T. A. G., Jackson, D. W. T., & Cooper, J. A. G. (2012). High resolution measured and modelled three-dimensional airflow over a coastal bowl blowout. *Geomorphology, 177–178*, 62–73. https://doi.org/10.1016/j.geomorph.2012.07.014

Sun, Y., Hasi, E., Liu, M., Du, H., Guan, C., & Tao, B. (2016). Airflow and sediment movement within an inland blowout in Hulun Buir sandy grassland, Inner Mongolia, China. *Aeolian Research, 22*, 13–22. https://doi.org/10.1016/j.aeolia.2016.05.002

Thomas, D. S. G. (2004). Dune, Coastal. In S. A. Goudie (Ed.), *Encyclopedia of geomorphology* (Vol. 1, pp. 291–297). Routledge.

Tripaldi, A. (2001). *Análisis sedimentológico de depósitos eólicos de valles intermontanos: su aplicación al estudio de secuencias terciarias del noroeste argentino*. Ph.D. Facultad de Ciencias Exactas y Naturales. Universidad de Buenos Aires, Argentina, 362 pp. http://digital.bl.fcen.uba.ar/Download/Tesis/Tesis_3428_Tripaldi.pdf